

Brain Composition in *Godyris zavaleta*, a Diurnal Butterfly, Reflects an Increased Reliance on Olfactory Information

Stephen H. Montgomery¹ and Swidbert R. Ott^{2*}

¹Department of Genetics, Evolution & Environment, University College London, London, UK, WC1E 6BT

²Department of Biology, University of Leicester, Leicester, UK, LE1 7RH

ABSTRACT

Interspecific comparisons of brain structure can inform our functional understanding of brain regions, identify adaptations to species-specific ecologies, and explore what constrains adaptive changes in brain structure, and coevolution between functionally related structures. The value of such comparisons is enhanced when the species considered have known ecological differences. The Lepidoptera have long been a favored model in evolutionary biology, but to date descriptions of brain anatomy have largely focused on a few commonly used neurobiological model species. We describe the brain of *Godyris zavaleta* (Ithomiinae), a member of a subfamily of Neotropical butterflies with enhanced reliance on olfactory information. We demonstrate for the first time the presence of sexually dimorphic glomeruli within a distinct macroglomerular complex (MGC) in the antennal lobe of a diurnal butterfly. This presents a striking convergence with the well-known moth MGC, prompting

a discussion of the potential mechanisms behind the independent evolution of specialized glomeruli. Interspecific analyses across four Lepidoptera further show that the relative size of sensory neuropils closely mirror interspecific variation in sensory ecology, with *G. zavaleta* displaying levels of sensory investment intermediate between the diurnal monarch butterfly (*Danaus plexippus*), which invests heavily in visual neuropil, and night-flying moths, which invest more in olfactory neuropil. We identify several traits that distinguish butterflies from moths, and several that distinguish *D. plexippus* and *G. zavaleta*. Our results illustrate that ecological selection pressures mold the structure of invertebrate brains, and exemplify how comparative analyses across ecologically divergent species can illuminate the functional significance of variation in brain structure. *J. Comp. Neurol.* 523:869–891, 2015.

© 2014 Wiley Periodicals, Inc.

INDEXING TERMS: adaptive brain evolution; comparative neuroanatomy; sexual dimorphism; antennal lobe; macroglomerular complex; Lepidoptera; Ithomiinae; *Godyris zavaleta*

The size and structure of nervous systems are shaped by selection in the context of developmental and functional constraints (Finlay and Darlington, 1995; Barton and Harvey, 2000; Striedter, 2005). Understanding how and to what extent selection negotiates these constraints to bring about adaptive evolutionary change that enhances the fitness of an animal's behavior is key to understanding the principles of brain evolution (Striedter, 2005). At the same time, such understanding can illuminate the function of brain components and neural networks. The principal way to tackling these questions has been to compare brain size and structure across multiple

S.H.M. is funded by a research fellowship from the Royal Commission of the Exhibition of 1851, with additional funding from the Linnean Society of London's Percy Sladen Memorial Fund, a Royal Society Research Grant (RG110466), and a British Ecological Society Early Career Project Grant. S.R.O. was supported by a University Research Fellowship from the Royal Society, London (UK).

This is an open access article under the terms of the Creative Commons Attribution-NonCommercial-NoDerivs License, which permits use and distribution in any medium, provided the original work is properly cited, the use is non-commercial and no modifications or adaptations are made.

*CORRESPONDENCE TO: Stephen H. Montgomery, Department of Genetics, Evolution & Environment, University College London, Gower Street, London, UK, WC1E 6BT. E-mail: Stephen.Montgomery@cantab.net

Received July 25, 2014; Revised October 17, 2014; Accepted November 4, 2014.

DOI 10.1002/cne.23711

Published online November 17, 2014 in Wiley Online Library (wileyonlinelibrary.com)

© 2014 Wiley Periodicals, Inc.

species with divergent ecologies (Felsenstein, 1985; Harvey and Pagel, 1998; Strausfeld, 2012). Studies of vertebrate brain evolution have benefited from large interspecific datasets (Stephan et al., 1981; Iwaniuk et al., 2004) to test hypotheses about developmental constraints (Barton and Harvey, 2000; Finlay and Darlington, 1995) and adaptive hypotheses concerning, for example, sensory adaptations (Barton et al., 1995) or social ecology (Dunbar, 1992). The assumptions and methods used in some of these studies have, however, been critiqued, along with calls for more experimental manipulation to support the results of comparative studies (Healy and Rowe, 2007).

The huge variety of ecological niches that invertebrates occupy, combined with their experimental tractability at the molecular, neurological, and environmental levels, provide rich opportunities for investigating the evolution of brains and behavior. However, comparative analyses in insects have so far largely focused on particular neural pathways or traits in a single or small number of model species (Brandt et al., 2005; Kurylas et al., 2008; El Jundi et al., 2009a,b; Kvello et al., 2009; Dreyer et al., 2010; Heinze and Reppert, 2012; Heinze et al., 2013). This work has identified potential adaptations to species-specific ecologies (Heinze and Reppert 2012; Heinze et al., 2013; El Jundi et al., 2009b; O'Donnell and Molina 2011; Streinzer et al., 2013) and environmentally induced plasticity (Withers et al., 1993; Snell-Rood et al., 2009; Ott and Rogers, 2010; Heinze et al., 2013). With some exceptions (e.g., Kondoh et al., 2003; Farris and Roberts, 2005; O'Donnell et al., 2011; Streinzer et al., 2013), these studies focused on specific questions concerning intraspecific variation, and as such any interspecific comparisons have considered distantly related species often with radically different ecologies.

The Lepidoptera have long been exploited as a model system for investigating both neurological (e.g., Bretschneider, 1924; Rospars, 1983) and evolutionary proc-

esses (e.g., Bates, 1862; Müller, 1879), and continue to be extensively studied from an ecological, phylogenetic, and, more recently, genomic (Xia et al., 2004; Zhan et al., 2011; Dasmahapatra et al., 2012) perspective. Detailed atlases of brain anatomy are currently available for three species of Lepidoptera: two night-flying moths, *Manduca sexta* (El Jundi et al., 2009b) and *Heliothis virescens* (Kvello et al., 2009), and one diurnal butterfly, *Danaus plexippus* (Heinze and Reppert, 2012). The morphology of the primary olfactory center, the antennal lobe, has been described for a greater number of species (Bretschneider, 1924; Boeckh and Boeckh, 1979; Rospars, 1983; Berg et al., 2002; Huetteroth and Schachtner, 2005; Masante-Roca et al., 2005; Skiri et al., 2005; Couton et al., 2009; Kazawa et al., 2009; Varela et al., 2009; Trona et al., 2010; Carlsson et al., 2013). Comparisons between these species, which diverged from a common ancestor ~100 MYA (Labandeira et al., 1994), reveal contrasting investment in sensory neuropil between night- and day-flying species, and a suite of traits apparently unique to *D. plexippus* that may be linked to a diurnal activity pattern, migratory behavior, or some other ecological variable (Heinze and Reppert, 2012; Heinze et al., 2013).

The relative size of different neuropil is thought to directly reflect their functional importance (Gronenberg and Hölldobler, 1999; El Jundi et al., 2009b; Wei et al., 2010; Heinze and Reppert, 2012). As such, the greater relative size of the visual neuropils in *D. plexippus*, and the smaller relative size of its olfactory neuropils, likely indicate a greater importance of visual information to diurnal butterflies (Hambäck et al., 2007). The enlarged volume of a small number of sexually dimorphic glomeruli in the antennal lobes of male moths (Rospars and Hildebrand, 1992; Huetteroth and Schachtner, 2005; El Jundi et al., 2009b; Löfaldli et al., 2010), but not butterflies (Rospars 1983; Heinze and Reppert 2012; Carlsson et al., 2013), can also be attributed to greater sensitivity for female pheromones

Abbreviations

AL	antennal lobe	MB	mushroom body
aMe	accessory medulla	MB-ca	mushroom body calyx
AN	antennal nerve	MB-lo	mushroom body lobes
AOTu	anterior optic tubercle	MB-pe	mushroom body peduncle
CB	central body	Me	medulla
CBL	lower central body	MGC	macro-glomeruli complex
CBU	upper central body	NGS	normal goat serum
CFN	central fibrous neuropil of AL	no	noduli
DMSO	dimethyl sulphoxide	NU	nodule unit of AOTu
Glom	glomeruli	oMe	outer medulla
HBS	HEPES-buffered saline	OR	olfactory receptor
HP	hair-pencils	OGC	optic glomerular complex
iMe	inner medulla	PA	pyrrolizidine alkaloids
iRim	inner rim of the lamina	PB	protocerebral bridge
La	lamina	PC	principal component
LAL	lateral accessory lobes	POTu	posterior optic tubercle
Lo	lobula	SP	strap of AOTu
LoP	lobula plate	UU	upper unit of AOTu
LU	lower unit of AOTu	ZnFA	zinc-formaldehyde solution

over large distances, with butterflies having lost this long-range function, instead using chemical communication on much smaller spatial scales (Rospars, 1983; Andersson et al., 2007; Carlsson et al., 2013).

However, like moths, butterflies respond to floral and host-plant related odors (Andersson and Dobson, 2003; Ômura and Honda, 2009; Carlsson et al., 2011, 2013), and chemical communication does play an important role in mating behavior (Scott, 1973; Andersson et al., 2007; Costanzo and Monteiro, 2007). The continued importance of olfaction in butterflies is further indicated by the similar numbers of olfactory receptor genes identified in the butterfly and moth genomes sequenced to date (Xia et al., 2004; Zhan et al., 2011; Dasmahapatra et al., 2012), and by the occurrence of sex-specific expression patterns of these genes in both groups (Nakagawa et al., 2005; Wanner et al., 2007; Briscoe et al., 2013). Conversely, some moths, including the crepuscular *M. sexta*, have greater visual acuity than others (Theobald et al., 2010) and may favor visual cues over olfactory cues when foraging (Raguso and Willis, 2005; Goyret et al., 2007).

To test the implied role of ecological selection pressures in shaping Lepidopteran brain structure we describe the brain of the Zavaleta Glasswing (*Godyris zavaleta*), a member of the Ithomiinae. Ithomiines are a Neotropical subfamily of nymphalid butterflies primarily studied for their Müllerian mimicry rings, where distantly related species converge on similar pigmentation patterns to better advertise their distastefulness to predators (Bates, 1862; Müller, 1879; Beccaloni, 1997). Transparent-winged ithomiines, such as *G. zavaleta*, typically remain in deeply shaded parts of their inner rainforest habitat (Pliske, 1975; Elias et al., 2008; Hill, 2010), raising the possibility of altered dependence on visual information, potentially in favor of olfactory cues.

A greater role for olfaction in *G. zavaleta* ecology is further suggested by their derived mating behavior. Ithomiines use pyrrolizidine alkaloids (PA) both as precursors for pheromone synthesis and for chemical protection (Pliske et al., 1976; Trigo and Motta, 1990). The majority of ithomiines obtain these PAs pharmacophagously as adults, by males feeding on the nectar of Boraginaceae and Asteraceae, or decomposing Boraginaceae leaves, in particular the genus *Heliotropium* (Brown, 1984; Trigo and Motta, 1990), to which males show a strong olfactory attraction (Pliske et al., 1976). Females obtain the derived defense compounds from males through the spermatophore (Brown, 1984), as part of a “nuptial gift”, potentially meaning pheromone production serves as an honest indicator of a male’s ability to collect PAs (Rutowski, 1984). Males secrete PA-derived pheromones on the costal margin of the hind-wing from a patch of specialized “hair-pen-

cils”. These hair-pencils are spread erect when a male is perching in an exposed area, or when in chase with another individual (Pliske, 1975a; Edgar et al., 1976; Pliske et al., 1976). Scent diffusion from hair pencils is thought to play a role in courtship (Müller, 1879; Gilbert, 1969; Drummond, 1976; Pliske et al., 1976; Haber, 1978; Kaye, 2009), by disseminating aphrodisiac pheromones (Pliske, 1975a) and attracting both sexes to multi-species leks (Haber, 1978). It may also function in male–male repellency and territorial marking (Pliske, 1975b; Edgar et al., 1976; Pliske et al., 1976; Vasconcellos-Neto and Brown, 1982). Chemical communication is therefore of heightened importance for ithomiines, both at close range and over larger spatial scales. Indeed, this pattern is predicted in Müllerian mimicry complexes: where visual communication cues may be unreliable, chemical communication can reduce male–male or interspecific pursuits (Brower et al., 1963; Scott, 1973).

In this article we test two hypotheses: 1) that the derived mating behavior, sex-specific motivation to locate PA sources, and sex-specific chemical communication mediated by hind-wing hair-pencils result in sexual dimorphism in the antennal lobes of *G. zavaleta* that is not observed in other butterflies; and 2) that the generally enhanced role of olfaction in *G. zavaleta* is supported by an investment in sensory neuropil intermediate between moths and *D. plexippus*. In addition, by describing the general layout of the brain we lay the foundations for future comparative studies across a greater number of species. Finally, Ithomiinae are the sister-clade to Danainae, the subfamily to which *D. plexippus* belongs (Freitas and Brown, 2004). The phylogenetic position of ithomiines therefore offers an improved comparison with *D. plexippus* to identify traits shared by diurnal species, or specific to either subfamily.

MATERIALS AND METHODS

Animals

Godyris zavaleta is not readily available from commercial breeders; therefore, all individuals were captured in the wild as part of a larger project to obtain samples across Ithomiinae. All individuals were captured in free flight, on the trails surrounding the Estación Científica Yasuní, in the Parque Nacional Yasuní, Orellana Province, Ecuador. Samples were collected during two field trips in November/December 2011 and September/October 2012 under collection permit no. 0033-FAU-MAE-DPO-PNY, and exported under permit nos. 001-FAU-MAE-DPO-PNY and 006-EXP-CIEN-FAU-DPO-PNY obtained from Parque Nacional Yasuní, Ministerio Del Ambiente, La Dirección Provincial de Orellana with cooperation from the Estación Científica Yasuní and

Pontificia Universidad Católica del Ecuador. *Godyris zavaleta* was the most abundant medium-sized species encountered across both field trips and in total eight males and eight females were included in the analyses. We assume all individuals were sexually mature, and that the age range is not biased between the sexes. In support of this, wing wear, a proxy for age (Walters et al., 2012), shows a similar range across both sexes. Wings and body tissue, stored in ethanol, were kept as voucher specimens.

Antibodies and sera for neuropil staining

We used indirect immunofluorescence staining against synapsin to reveal the neuropil structure of the brain under a confocal microscope (Ott, 2008). This technique exploits the abundant expression of synapsin, a vesicle-associated protein, at presynaptic sites. Monoclonal mouse anti-synapsin antibody 3C11 (anti-SYNORF1; Klagges et al., 1996) was obtained from the Developmental Studies Hybridoma Bank (DSHB; University of Iowa, Department of Biological Sciences, Iowa City, IA; RRID: AB_2315424). 3C11 immunostaining has been used as an anatomical marker of synaptic neuropil in a wide range of arthropod species. The 3C11 antibody was raised against a bacterially expressed fusion protein generated by adding a glutathione S-transferase (GST)-tag to a cDNA comprising most of the 5' open reading frame 1 of the *Drosophila melanogaster* synapsin gene (*Syn*, CG3985). The binding specificity of this antibody has been characterized in *D. melanogaster* by Klagges et al. (1996) and the epitope was later narrowed down to within LFGGMEVCGL in the C domain (Hofbauer et al., 2009). This motif is highly conserved across arthropod synapsins.

For the present study we confirmed its presence in the synapsin ortholog of *D. plexippus* by bioinformatics analysis using Ensembl Genomes (<http://www.ensemblgenomes.org>). We used the *D. melanogaster* synapsin isoform F amino acid sequence (*Syn1*; UniProt Q24546-1) as a query for *blastp* (v.2.0MP) searches on predicted proteins in the *D. plexippus* genome (DanPle_1.0, INSDC assembly GCA_000235995.1; Zhan et al., 2011). This identified a predicted 692 AA protein from hypothetical gene KGM_17479 as the *Syn1* ortholog in *D. plexippus* (53.95% identity over the region corresponding to amino acid residues 3–581 in *Syn1*; $e = 1.4e-153$). The 3C11 epitope motif occurs as IFGGLEVCAL in *D. plexippus*. We subsequently obtained the ortholog of this locus in *Bombyx mori* (XP_004932024.1) using a *blastp* search against the *B. mori* genome (ASM15162v1, INSDC Assembly GCA_000151625.1; Xia et al., 2004), the most distantly related Lepidopteran genome available, to assess the conservation of the motif across Lepidoptera.

The 3C11 epitope motif shows 100% identity between *B. mori* and *D. plexippus*, suggesting it is very highly conserved. The staining pattern obtained with 3C11 in *G. zavaleta* is highly similar to that in *D. plexippus* and other Lepidoptera (El Jundi et al., 2009b; Kvello et al., 2009; Heinze and Reppert, 2012). Cy2-conjugated affinity-purified polyclonal goat antimouse IgG (H+L) antibody (Jackson ImmunoResearch Laboratories, West Grove, PA) was obtained from Stratech Scientific (Newmarket, Suffolk, UK; Jackson ImmunoResearch Cat No. 115-225-146, RRID: AB_2307343).

Immunocytochemistry

Brains were fixed and stained following a published protocol (Ott, 2008) previously applied to a range of invertebrates including the monarch butterfly, *D. plexippus* (Heinze and Reppert, 2012). The protocol was divided into two stages, the first of which was performed at the Estación Científica Yasuní. Briefly, the brain was exposed under HEPES-buffered saline (HBS; 150 mM NaCl; 5 mM KCl; 5 mM CaCl₂; 25 mM sucrose; 10 mM HEPES; pH 7.4) and fixed in situ for 16–20 hours at room temperature (RT) in zinc-formaldehyde solution (ZnFA; 0.25% [18.4 mM] ZnCl₂; 0.788% [135 mM] NaCl; 1.2% [35 mM] sucrose; 1% formaldehyde) under agitation. Fixation with ZnFA affords considerably better antibody penetration, staining intensity, and preservation of morphology than conventional (para)formaldehyde fixation (Ott, 2008; Heinze and Reppert, 2012). The brain was subsequently dissected out, under HBS, by removing the eye cuticle in slices before gently plucking away the main body of the ommatidia to reveal the basement membrane. The basement membrane of the retina is firmly attached to the lamina, which itself is loosely connected to the rest of the optic lobe. The most successful method to remove the retina was to use a very fine pair of tweezers to cut small sections away from the lamina, rather than to try and pull strips away. After removing the retina, and any air sacks or tissue around the outer surface of the brain, the brain was lifted from the head capsule, washed three times in HBS, and placed into 80% methanol/20% DMSO for a minimum of 2 hours under agitation. The brain was then transferred to 100% methanol and stored at RT. After transportation back to the UK samples were stored at -20°C .

In the second stage of the protocol, performed in laboratory conditions in the UK, the samples were brought to RT and rehydrated in a decreasing methanol series (90%, 70%, 50%, 30%, 0% in 0.1 M Tris buffer, pH 7.4, 10 minutes each). Normal goat serum (NGS; New England BioLabs, Hitchin, Hertfordshire, UK) and antibodies were diluted in 0.1 M phosphate-buffered saline (PBS; pH 7.4) containing 1% DMSO and 0.005% NaN₃ (PBSd).

Nonspecific antibody binding was blocked by preincubation in 5% NGS (PBSD-NGS) for 2 hours at RT. Antibody 3C11 was then applied at a 1:30 dilution in PBSD-NGS for 3.5 days at 4°C under agitation. The brains were rinsed in PBSD for 3 × 2 hours before applying the Cy2-conjugated antimouse antibody 1:100 in PBSD-NGS for 2.5 days at 4°C under agitation. This was followed by a series of increasing concentrations (1%, 2%, 4% for 2 hours each, 8%, 15%, 30%, 50%, 60%, 70%, and 80% for 1 hour each) of glycerol in 0.1 M Tris buffer with DMSO to 1%. The brains were then passed in a drop of 80% glycerol directly into 100% ethanol and agitated for 30 minutes; the ethanol was changed three times with 30-minute incubations. Finally, to clear the tissue, the ethanol was underlain with methyl salicylate, the brain was allowed to sink, before the methyl salicylate was refreshed twice with 30-minute incubations.

Confocal imaging

Samples were mounted in fresh methyl salicylate between two round coverslips separated by a thin metal washer (UK size M8 or M10). All imaging was performed on a confocal laser-scanning microscope (Leica TCS SP8, Leica Microsystem, Mannheim, Germany) at the University College London Imaging Facility, using a 10× dry objective lens with a numerical aperture of 0.4 (Leica Material No. 11506511, Leica Microsystem). In each individual brain, we captured a single stack of confocal images from one antennal lobe, and a series of overlapping stacks of lower resolution that together covered the whole brain. For the antennal lobe stack, we randomly selected either the left or the right antennal lobe and imaged it with a mechanical z-step of 1 μm, an x-y resolution of 1024 × 1024 pixels, and a line average of six. For the whole brain imaging, we used a mechanical z-step of 2 μm with an x-y resolution of 512 × 512 pixels. Imaging the whole brain required 2 × 2 stacks in the x-y dimensions with an overlap of 10%; the tiled stacks were automatically merged in Leica Applications Suite Advanced Fluorescence software. Each brain was scanned from the posterior and anterior side to span the full z-dimension of the brain. These two image stacks were subsequently merged in Amira 3D analysis software 5.5 (FEI Visualization Sciences Group), using a custom module "Advanced Merge" provided by Rémi Blanc (Application Engineer at FEI Visualization Sciences Group). This module combines a sequence of other modules: the two stacks are aligned using affine registration and subsequently merged to produce the combined stacks. The merging procedure resampled the first third of the anterior image stack, the final third of the posterior image stack, and averaged the intervening images. Finally, to

correct for the artifactually shortened z-dimension associated with the 10× air objective, a correction factor of 1.52 was applied to the voxel size in the z-dimension. This correction factor was obtained during the analysis of the *D. plexippus* brain using identical methods (Heinze and Reppert, 2012; S. Heinze, pers. comm.). Images presented in the figures to illustrate key morphological details were captured separately as single images.

Neuropil segmentations and volumetric reconstructions

Neuropils were reconstructed from the confocal image stacks in Amira 5.5. We assigned image regions to anatomical structures in the Amira *labelfield* module by defining outlines based on the brightness of the synapsin immunofluorescence. This process segments the image into regions that are assigned to each particular structure and regions that are not. Within each stack, every third image was manually segmented in this way using the outline or magic-wand tool. The segmentation was then interpolated in the z-dimension across all images that contain the neuropil of interest. The neuropil outlines were then fine-edited in all three dimensions and smoothed. The *measure statistics* module was used to determine volumes (in μm³) for each neuropil. 3D polygonal surface models of the neuropils were constructed from the smoothed labelfield outlines using the *SurfaceGen* module.

As explained in the previous section, in each of the $n = 8$ male and $n = 8$ female brains, either the left or the right antennal lobe was randomly chosen for imaging at higher resolution (1024 × 1024 pixel, 1.52 μm optical z-sampling). These high-resolution antennal lobe stacks were used to measure the following variables (yielding one value per brain for each variable, i.e., $N = 16$): 1) the volumes of the four glomeruli that form a distinct cluster below the base of the antennae, and that we hypothesize may be functionally analogous to the macroglomerular complex (MGC) observed in moths; 2) the volumes of seven "ordinary" glomeruli that could be reliably identified by their size, position, and shape; 3) the total volume of all glomeruli and of the entire antennal lobe including the central fibrous neuropil. In addition, in a subset of two males and two females the total number of glomeruli in one antennal lobe was estimated by individually segmenting all discernable glomeruli in the antennal-lobe stack and counting their number. Difficulty in identifying the boundaries between closely packed glomeruli likely causes some measurement error.

The whole-brain composite stacks (assembled from the lower-resolution 512 × 512 pixel scans with 3.04 μm optical z-sampling) were used to reconstruct and

TABLE 1.
Mean Volumes of Major Neuropil

Neuropil	Mean ($N = 16$) ¹	SD	Relative SD (%)	Asymmetry		Sexual dimorphism			
				Raw volume		Raw volume		% volume	
				t_{15} ²	P	t_{14}	P	t_{14}	P
Lamina	2.31×10^7	5.70×10^6	24.70	0.31	0.766	-3.82	0.003	-1.72	0.114
Medulla	6.96×10^7	1.47×10^7	21.11	0.02	0.985	-2.07	0.057	-1.11	0.288
Accessory medulla	6.88×10^4	1.43×10^4	20.71	0.32	0.754	0.43	0.676	2.79	0.015
Inner lobula	8.07×10^6	1.30×10^6	16.06	0.12	0.905	-0.73	0.478	1.27	0.229
Lobula plate	5.27×10^6	1.33×10^6	25.31	0.33	0.749	-0.58	0.573	0.26	0.803
Antennal lobes	8.54×10^6	1.92×10^6	22.45	1.48	0.159	-0.54	0.601	0.98	0.343
AOTu	1.01×10^6	2.90×10^5	28.66	0.52	0.613	-2.52	0.025	-2.71	0.018
MB calyx	2.40×10^6	6.37×10^5	26.55	0.20	0.843	-1.14	0.273	-0.27	0.795
MB peduncle	2.29×10^5	7.34×10^4	32.10	0.73	0.476	-1.16	0.265	-0.07	0.945
MB lobes	1.33×10^6	3.79×10^5	28.54	0.14	0.888	-0.57	0.58	0.56	0.585
Central body lower	1.78×10^5	5.71×10^4	32.04	—	—	-1.03	0.32	0.30	0.774
Central body upper	6.32×10^5	1.64×10^5	25.94	—	—	-0.76	0.457	-0.06	0.95
Noduli	1.89×10^4	9.22×10^3	48.80	0.80	0.439	-0.79	0.46	-0.48	0.649
Protocerebral bridge	9.79×10^4	2.51×10^4	25.63	0.56	0.584	-0.19	0.849	0.65	0.527
POTu	2.00×10^4	7.57×10^3	37.93	1.21	0.245	1.24	0.248	1.92	0.077
Total mid brain	8.30×10^7	1.90×10^7	22.91	—	—	-1.89	0.079	—	—

¹For paired structures the mean is calculated from the combined volume of left and right neuropil

²Lower sample sizes for the lamina due to damage caused when removing the retina, and lack of clear boundaries for the noduli reduced the sample size to 12 (t_{11}) in both cases

measure five paired neuropils in the optic lobes, and seven paired and two unpaired neuropils in the midbrain. All paired neuropils (including the antennal lobes) were measured on both sides of the brain to permit tests of asymmetry, yielding two paired measurements per brain (i.e., $N = 16 \times 2$) for each structure. In each brain, both antennal lobes were measured at this lower voxel resolution; the value obtained in the higher-resolution antennal-lobe stacks was not reused in this analysis in order to permit unbiased comparisons between the two sides and with other structures. In addition, we measured the total neuropil volume of the midbrain to control for allometric differences. In Lepidoptera the subesophageal ganglion is fused tightly against the ventroposterior boundary of the supraesophageal ganglion (i.e., against what is referred to as the "midbrain" in insects with less extensively fused head ganglia such as Orthoptera; Kurylas et al., 2008), resulting in a single compact central mass that is flanked by the protocerebral optic lobes. In keeping with the earlier Lepidopteran literature, we use the term "midbrain" for this fused central mass, which thus comprises: the protocerebral neuromere excluding the optic lobes; the deuto- and tritocerebral neuromeres; and the subesophageal neuromeres. All data collection was performed blind with respect to the sex of the individual. The color code used for the neuropils in the 3D models is consistent with previous neuroanatomical studies of invertebrate brains (Brandt et al., 2005; Kurylas et al., 2008; El Jundi et al., 2009a,b; Dreyer et al., 2010; Heinze and Reppert, 2012).

Statistical analysis

Paired two-tailed t -tests on combined data from males and females were used to test for left-right asymmetry (16×2 paired observations from $n = 16$ individuals, 15 degrees of freedom, except in a small number of cases where one side was damaged) (Table 1). The normality of each dataset was examined using a Shapiro-Wilk test and where any dataset within a set of analyses was found to deviate from normality, the analyses were repeated using a nonparametric Mann-Whitney test. In all cases parametric and nonparametric tests led to the same conclusions, so we only present results from the parametric test. All statistical analyses were performed in GenStat (VSNi, Hemel Hempstead, UK) or R (R Development Core Team, 2008). We found no evidence for asymmetry in the volume of paired neuropil (Table 1) and subsequently summed their volumes to calculate the total volume of a structure. Unpaired two-tailed two-sample t -tests were used to test for sexual dimorphism ($n = 8$ males and $n = 8$ females, total $N = 16$, 14 degrees of freedom); for paired neuropils, the tests were carried out on the sum of the left and right volume.

We collected published data for neuropil volumes of three other Lepidoptera; the monarch butterfly (*D. plexippus*; Heinze and Reppert, 2012), the giant sphinx moth (*M. sexta*; El Jundi et al., 2009b), and the tobacco budworm moth (*Heliothis virescens*; Kvello et al., 2009). Data were available for eight neuropils across all three species (Table 3). We calculated the relative investment

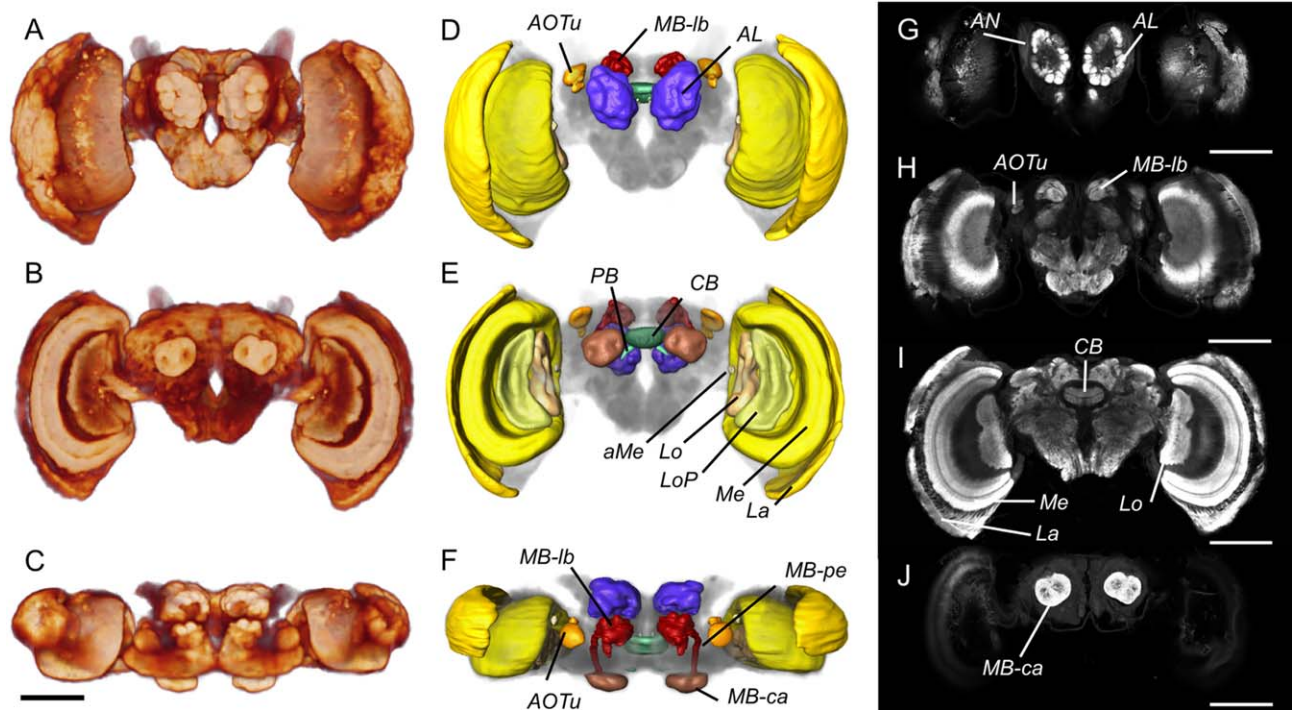


Figure 1. Overview of the anatomy of the *G. zavaleta* brain. **A–C:** Volume rendering of synapsin (3C11) immunofluorescence showing the surface morphology of the brain neuropil from the anterior (A), posterior (B), and dorsal (C) view. **D–F:** Surface reconstructions of the major neuropil compartments from the anterior (D), posterior (E), and dorsal (F) view. The midbrain houses the antennal lobes (AL) which lie at the base of the antennal nerve (AN in G), the anterior optic tubercles (AOTu), the central body (CB), protocerebral bridge (PB), and the mushroom body, which comprises the calyx (MB-ca), peduncle (MB-pe), and lobes (MB-lb); the optic lobes comprise the lamina (La), medulla (Me), and accessory medulla (aMe), the lobula (Lo), and lobula plate (LoP). **G–J:** Anti-synapsin immunofluorescence in frontal confocal sections taken at progressively more posterior levels. G: The antennal lobes (AL) are the most anterior midbrain neuropils. H: Further back, the anterior optic tubercles (AOTu) flank the mushroom body lobes (MB-lb), which occupy a dorsomedial position. I: The central body (CB) and the three main neuropils in the optic lobe, the lamina (La), medulla (Me), and lobula (Lo). J: The mushroom body calyx (MB-ca) at the back end of the midbrain. The individual displayed is female. Scale bars = 500 μ m.

in each neuropil by comparing its volume to the total neuropil volume of either the whole brain, or of only the midbrain. As the volume of the lamina was not measured in *H. virescens* the "whole brain" excludes lamina volume in order to make the data comparable across species. Differences in brain architecture across species were identified by multivariate principal component analysis of these data, and visualized as biplots (Greenacre, 2010) in R package *ggbiplot* (V.Q. Vu, <https://github.com/vqv/ggbiplot>).

Relative size was measured in two ways. First, by calculating the volume of each structure as a percentage of the total, or total midbrain, neuropil. Second, by calculating the residuals of a phylogenetically corrected least squares linear regression between each structure and the rest of the brain. For this analysis, a phylogeny of the four species was created using data on two loci, *COI* and *EF1a* (GenBank Accession IDs, *COI*: EU069042.1, GU365908.1, JQ569251.1, JN798958.1; *EF1a*: EU069147.1, DQ157894.1, U20135.1, KC893204.1). The

data were aligned and concatenated using MUSCLE (Edgar, 2004), before constructing a maximum likelihood tree in MEGA v.5 (Tamura et al., 2011). Phylogenetically controlled regressions were performed between log-transformed data in BayesContinuous in BayesTraits (freely available from www.evolution.rdg.ac.uk; Pagel, 1999) using this phylogeny.

These two approaches to calculating relative size make different assumptions about the underlying interspecific allometric relationships and their functional interpretation (Montgomery, 2013). Using percentage volumes assumes a 1:1 allometric relationship, which is rarely the case, and does not account for the nonindependence of data. Changes in percentage size may therefore reflect differences in overall investment, but not necessarily adaptive changes in function if the true allometric relationship reflects a constraint, while changes in residual size suggest changes in the underlying functional relationship between two regions of the brain (Montgomery, 2013). In the present analysis the sample size available for

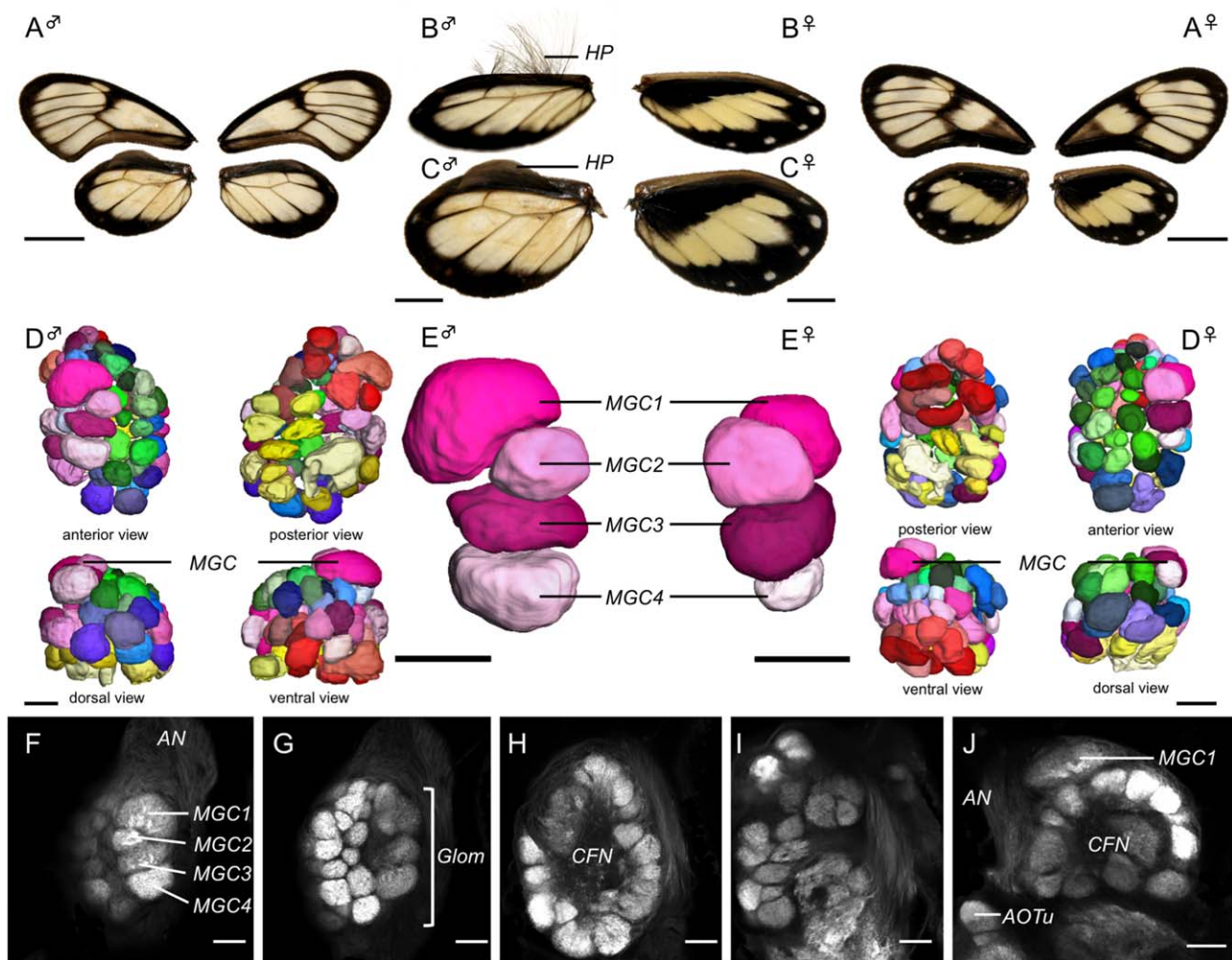


Figure 2. Sexual dimorphism in the wings and antennal lobes (AL). **A–C:** Wing morphology in males (♂) and females (♀) showing wing pigmentation on the dorsal surface (A) and the presence of hair-pencils (HP) on the hind wings of males from an oblique anterodorsal view (B) and a direct dorsal view (C). **D,E:** Surface reconstructions of the full complement of AL glomeruli (D), and of the subset of four glomeruli that form the macroglomerular complex (MGC1–4 in E). Among the ordinary glomeruli, green tones indicate the dorsalmost glomeruli, blue tones the middle layer, pink tones the posterior layer, red tones the posterodorsal glomeruli and yellow tones the posteromedial glomeruli. **F–J:** Synapsin immunofluorescence in single confocal sections of the AL. **F–I:** Frontal sections that move progressively deeper into the AL until reaching its posterior boundary. The four distinct glomeruli of the MGC (MGC1–4 in F) occupy the most anterior position in the AL, close to the root of the antennal nerve (AN in F). The ordinary glomeruli (Glom in G) surround the central fibrous neuropil (CFN in H,J). **J:** A horizontal section at the level of the anterior optic tubercle (AOTu) and shows MGC1 protruding from the general spherical shape of the AL. Scale bars = 1.0 cm in A; 0.5 cm in B,C; 50 μ m in D–J.

determining the allometric relationships is quite low, which limits the accuracy of the residual estimates. However, both analyses led to similar conclusions.

RESULTS

General layout of the *Godyris* brain

The general layout of the brain in *G. zavaleta* is similar to that of other Lepidoptera (El Jundi et al., 2009b; Kvello et al., 2009; Heinze and Reppert, 2012). The subesophageal ganglion is fused against the ventroposterior boundary of the supraesophageal ganglion, resulting in a

single compact mass, with the esophagus running through a large central aperture. This single medial mass, which we henceforth refer to as the "midbrain," is separated from the flanking optic lobes by pronounced lateral isthmuses on either side (Fig. 1). As expected, synapsin immunostaining resulted in intense fluorescence in regions of synaptic neuropil and little or no fluorescence in fiber tracts and in the cell body cortex. The boundaries of most previously identified neuropil structures were clearly defined, permitting segmentation of five paired neuropils in the optic lobes, and seven paired

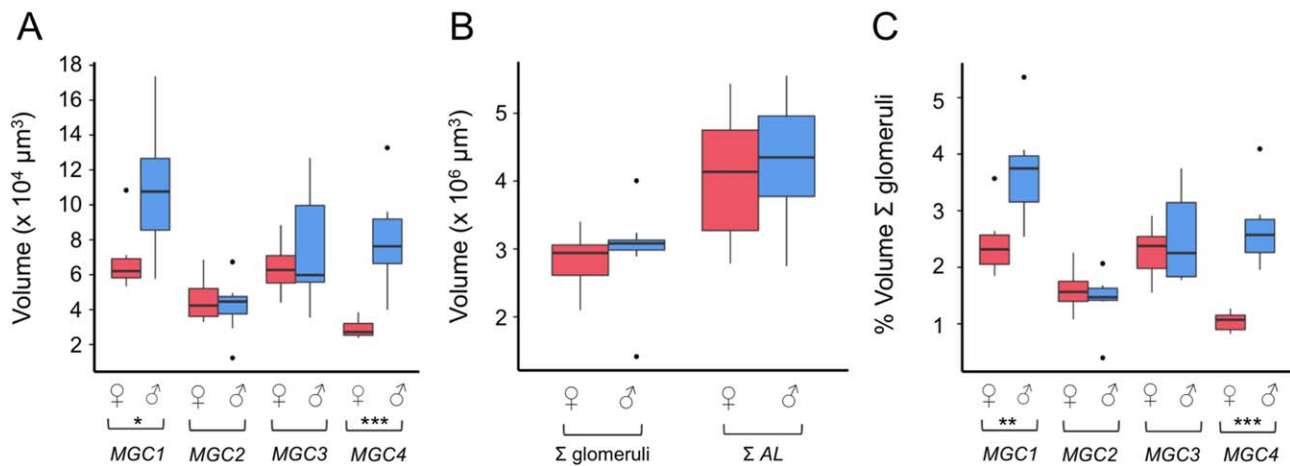


Figure 3. Volumetric quantification of the sexual dimorphism in the antennal lobes. **A:** Raw volumes of MGC1–4 for males (♂) and females (♀). **B:** Raw volumes of the total volume of all glomeruli and the AL (including the CFN) for males (♂) and females (♀). **C:** Volumes of MGC1–4 for males (♂) and females (♀) as a proportion of the total volume of the glomeruli. The boxplots show the median (horizontal line in box), the interquartile range (range of the box), and the maximum and minimum of the range (whiskers); outliers are shown as separate data points. Significant differences between males and females are indicated by * $P < 0.05$, ** $P < 0.01$, *** $P < 0.001$.

and two unpaired neuropils in the midbrain. We quantified the volumes of these 14 neuropils in eight males and eight females (Table 1). A large proportion of the midbrain lacks distinct internal boundaries and we therefore did not segment it into subdivisions in our analysis.

Antennal lobes

The general morphology of the antennal lobes (Fig. 2; AL in Fig. 1C,F) is similar to that in other Lepidoptera (Huetteroth and Schachtner, 2005; El Jundi et al., 2009b; Heinze and Reppert, 2012). In *G. zavaleta* each AL contains on average 67 glomeruli ($N = 2♂: 70, 63, 2♀: 67, 68$), globular units of neuropil arranged around a central fibrous neuropil (CFN in Fig. 2H,J). In *G. zavaleta* four large glomeruli at the root of the antennal nerve (AN in Fig. 2F,J) form a distinct unit that is raised with respect to the anterior surface of the AL (Fig. 2E). The position of this unit closely matches that of the sexually dimorphic MGC present in moths, which has known roles in sex pheromone detection (Hansson et al., 1991; Todd et al., 1995; Berg et al., 1998). We label these glomeruli MGC subunits 1–4 (MGC1–4), with MGC1 being the dorsal most glomerulus. While we hypothesize that they may be involved in pheromone signaling in Ithomiinae, we emphasize that we use "MGC" as a purely descriptive morphological term that does not imply homology with the MGC of moths.

In *D. plexippus* two large glomeruli, which lie in a similar position, appear morphologically distinct from other "normal glomeruli" in shape and internal appearance (Heinze and Reppert, 2012). Whereas the volumes

of this pair of glomeruli cannot be distinguished between the sexes in *D. plexippus* (Heinze and Reppert, 2012), there is a clear signature of sexual dimorphism in the volume of the MGC in *G. zavaleta* (Fig. 3, ♂ vs. ♀). In absolute terms, the total volume of MGC1–4 is significantly larger in males than females ($t_{14} = 2.69$, $P = 0.018$). This difference is driven by two sexually dimorphic MGC glomeruli (Fig. 3A, Table 2), MGC1 ($t_{14} = 2.82$, $P = 0.014$) and MGC4 ($t_{14} = 4.97$, $P = 0.001$), both of which are larger in males (by ~60% and 170%, respectively) where they are the largest of the glomeruli, approximately two standard deviations from the average glomerular volume. This sexual dimorphism mirrors the sexually dimorphic hind-wing hair pencils (Fig. 2A–C). The volumes of MGC2 ($t_{14} = 0.45$, $P = 0.650$) and MGC3 ($t_{14} = 0.84$, $P = 0.414$) are not significantly different between males and females, neither are seven control glomeruli (Table 2a). There was no significant sex difference in the sum total volume of all glomeruli ($t_{14} = 0.54$, $P = 0.598$) or in the total volume of the whole AL ($t_{14} = 0.44$, $P = 0.668$) (Fig. 3B). This suggests that strong size dimorphism is limited to a subset of glomeruli, although we cannot rule out subtle sex differences in glomerular size outside the MGC. The similar sum total volumes of the glomeruli in the two sexes do not, however, by themselves indicate that some other, non-MGC glomeruli are necessarily larger in females, because MGC1 and MGC4 together account for only 3.56% and 6.37% of the total volume of all glomeruli in females and males, respectively. If there were no other sex differences in glomerular size or number, the larger MGC in males would increase the

TABLE 2.

Statistical Support for the Presence of Sexually Dimorphic Glomeruli

a) Raw volumes of MGC and control glomeruli, total glomeruli and total AL volume						
	Male		Female		Sexual dimorphism	
	mean volume (x 10 ⁴ μm ³)	SD (x 10 ⁴ μm ³)	mean volume (x 10 ⁴ μm ³)	SD (x 10 ⁴ μm ³)	t ₁₄	P
MGC1	10.980	3.856	6.756	1.751	-2.82	0.014
MGC2	4.184	1.594	4.512	1.215	0.45	0.650
MGC3	7.503	3.302	6.419	1.539	-0.84	0.414
MGC4	7.971	2.809	2.934	0.578	-4.97	0.001
Control glomerulus 1	1.947	0.405	2.366	0.679	1.50	0.157
Control glomerulus 2	3.371	1.229	3.672	0.692	0.60	0.555
Control glomerulus 3	2.018	0.786	1.795	0.433	-0.62	0.545
Control glomerulus 4	3.235	1.058	3.446	1.027	0.37	0.714
Control glomerulus 5	4.870	1.538	3.877	0.695	-1.66	0.118
Control glomerulus 6	2.762	1.011	2.351	1.212	-0.74	0.474
Control glomerulus 7	0.894	0.219	1.106	0.243	1.84	0.087
Total glomeruli	297.800	71.860	281.800	43.114	-0.54	0.600
Total antennal lobe	431.000	94.773	409.700	98.553	-0.44	0.670

b) Sexual dimorphism in MGC is robust to variation in total AL size						
	Male		Female		Sexual dimorphism	
	mean % of Σ glomeruli	SD	mean % of Σ glomeruli	SD	t ₁₄	P
MGC1	3.692	0.861	2.413	0.540	-3.56	0.003
MGC2	1.439	0.473	1.607	0.362	0.79	0.441
MGC3	2.49	0.766	2.29	0.448	-0.66	0.519
MGC4	2.68	0.661	1.05	0.172	-6.77	<0.001

	Male		Female		Sexual dimorphism	
	mean % of Σ AL	SD	mean % of Σ AL	SD	t ₁₄	P
MGC1	2.580	0.864	1.670	0.280	-2.81	0.022
MGC2	0.990	0.333	1.120	0.211	0.95	0.360
MGC3	1.680	0.417	1.580	0.208	-0.61	0.550
MGC4	1.882	0.692	0.740	0.163	-4.55	<0.001

total by only 3.00%; this differential contribution is likely to be drowned out by interindividual variation, which is 19.96% of the mean volume. When the size of each of the four MGC glomeruli is considered as a proportion of either the total volume of all glomeruli (Fig. 3C) or of the whole antennal lobe, sexual dimorphism is again limited to MGC1 and MGC4 (Table 2b). No other neuropil was found to be consistently sexually dimorphic either before or after accounting for differences in the overall size of the midbrain (Table 1).

Visual neuropil

Five major neuropils are clearly visible in the optic lobes (Fig. 4), each well defined and clearly homologous to those observed in other Lepidoptera. The outermost, the lamina, forms a thin "cap" to the rest of the optic

lobe, separated from it by the first optic chiasm (La in Figs. 1D,E,I, 4A-D,G). Next, the medulla forms a thicker, layered structure (Me in Figs. 1E,I, 4A-E,G) with two major divisions, the outer and inner layer (oMe, iMe in Fig. 4G), each of which contains a further number of striations (~10 in total across the Me). Tucked against the anteromedial edge of the medulla is the small but distinct accessory medulla (aMe in Figs. 1E, 4A,B,D). Finally, the lobula and lobula plate form a pair of neuropil neighboring one another along the anterior/posterior axis (Lo in Figs. 1E,I, 4A-C,E,M; LoP in Figs. 1E, 4A,B,D).

Heinze and Reppert (2012) noted a number of unusual features in the optic lobes of *D. plexippus* that may reflect adaptations to their general ecology or perhaps specifically to their migratory behavior. First, they observed an inner rim of intense synapsin staining in

TABLE 3.
Volumes of Main Neuropil in Four Lepidoptera

Neuropil	Godyris zavaleta			Danaus plexippus			Heliothis virescens			Manduca sexta		
	abs. (μm^3)	% Σ neuropil ¹	% Σ midbrain	abs. (μm^3)	% Σ neuropil ¹	% Σ midbrain	abs. (μm^3)	% Σ neuropil ¹	% Σ midbrain	abs. (μm^3)	% Σ neuropil ¹	% Σ midbrain
Antennal lobe ²	8.540×10^6	4.99	10.29	1.559×10^7	3.14	9.41	1.274×10^7	8.64	11.38	6.780×10^7	8.33	15.80
AOT	1.011×10^6	0.59	1.22	3.659×10^6	0.74	2.21	9.980×10^5	0.68	0.89	4.358×10^6	0.54	1.02
Peduncle + lobes	1.558×10^6	0.91	1.88	9.678×10^6	1.95	5.84	2.750×10^6	1.86	3.42	1.467×10^7	1.80	3.42
Calyx	2.398×10^6	1.40	2.89	1.274×10^7	2.57	7.69	4.760×10^6	3.23	4.33	1.859×10^7	2.28	4.33
Central body	8.099×10^5	0.47	0.98	2.387×10^6	0.48	1.44	1.690×10^6	1.15	1.03	4.415×10^6	0.54	1.03
Medulla	6.957×10^7	40.65	—	2.782×10^8	55.99	—	2.570×10^7	17.42	—	2.800×10^8	34.40	—
Lobula	1.334×10^7	7.79	—	3.506×10^7	7.06	—	7.010×10^6	4.75	—	6.295×10^7	7.73	—
Lobula plate	5.273×10^6	3.08	—	1.791×10^7	3.61	—	2.850×10^6	1.93	—	4.185×10^7	5.14	—
Total midbrain	8.298×10^7	48.48	—	1.657×10^8	33.34	—	1.119×10^8	75.89	—	4.292×10^8	52.73	—
Total neuropil	1.712×10^8	—	—	4.968×10^8	—	—	1.475×10^8	—	—	8.140×10^8	—	—

¹Volumes expressed as a percentage of the total neuropil volume excluding the lamina, which was not measured in *H. virescens*.

²For *Heliothis* the AL was measured without the CFN, the data presented are "corrected" to estimated total AL volume using the ratio of total glomerular volume/total AL volume from *G. zavaleta*. This correction does not affect the results of interspecific analyses.

the lamina. This inner rim is also observed in *G. zavaleta* (iRim in Fig. 4G). Second, they noted a small, irregularly shaped neuropil running ventrally alongside the medial edge of the medulla to the accessory medulla. In some *G. zavaleta* individuals thin projections can be seen connecting the medulla and accessory medulla, but they are not as well defined as they appear in *D. plexippus*. Third, and most strikingly, Heinze and Reppert (2012) identified a large neuropil, the optic glomerular complex (OGC), located in the optic stalk, stretching from the medial margin of the lobula to the lateral edge of the mushroom body calyx. This neuropil is not observed in *G. zavaleta*. However, we do observe a small but distinct, brightly stained neuropil at the medial margin of the lobula (asterisk, Fig. 4M) that is not mentioned in Heinze and Reppert's (2012) thorough description of the *D. plexippus* brain. Whether or not this is a homologous structure to the OGC that has been expanded in *D. plexippus* is unclear.

Within the midbrain, the paired anterior optic tubercle (AOTu) are important visual neuropils that receive afferent projections from the medulla and lobula (Homberg et al., 2003). As in *D. plexippus* (Heinze and Reppert, 2012) the AOTu in *G. zavaleta* (Figs. 1D,F,H, 4C,D) can be subdivided into four units: a large upper unit (UU) and three smaller units, the lower unit (LU), the nodular unit (NU), and the strap (SP), which connects LU and NU (Fig. 4H–L). The presence of the strap in both species suggests that it is not specifically linked to long-distance navigation. Rather, it may be a butterfly synapomorphy, since moths reportedly lack the strap (Heinze and Reppert, 2012). A further distinctive feature of the AOTu of both butterfly species is an expansion of the upper unit, first reported in *D. plexippus* by Heinze and Reppert (2012). This expansion is less extreme in *G. zavaleta*. In *M. sexta* the ratio of upper unit : lower unit : nodular unit is 73: 10: 17, in *G. zavaleta* it is 85: 4: 11, and in *D. plexippus* it is 93: 2: 5. This pattern of expansion matches corresponding differences in medulla size, suggesting this is a potential case of coevolution between functionally related neuropil (Barton and Harvey, 2000).

Mushroom bodies

The mushroom bodies are integral to higher-order information processing, learning, and memory (Farris, 2005; Strausfeld et al., 2009). As in other insects, the mushroom body in *G. zavaleta* (Fig. 5) can be divided into three major substructures: the calyx (MB-ca in Figs. 1E,F,J, 5), the pedunculus (MB-pe in Figs. 1F, 5), and the lobe system (MB-lb in Figs. 1D,F,H, 5). The mushroom bodies are well developed in *G. zavaleta* but both the lobes and calyx are notably smaller than in *D. plexippus* (Table 3). Moreover, unlike in *D. plexippus*,

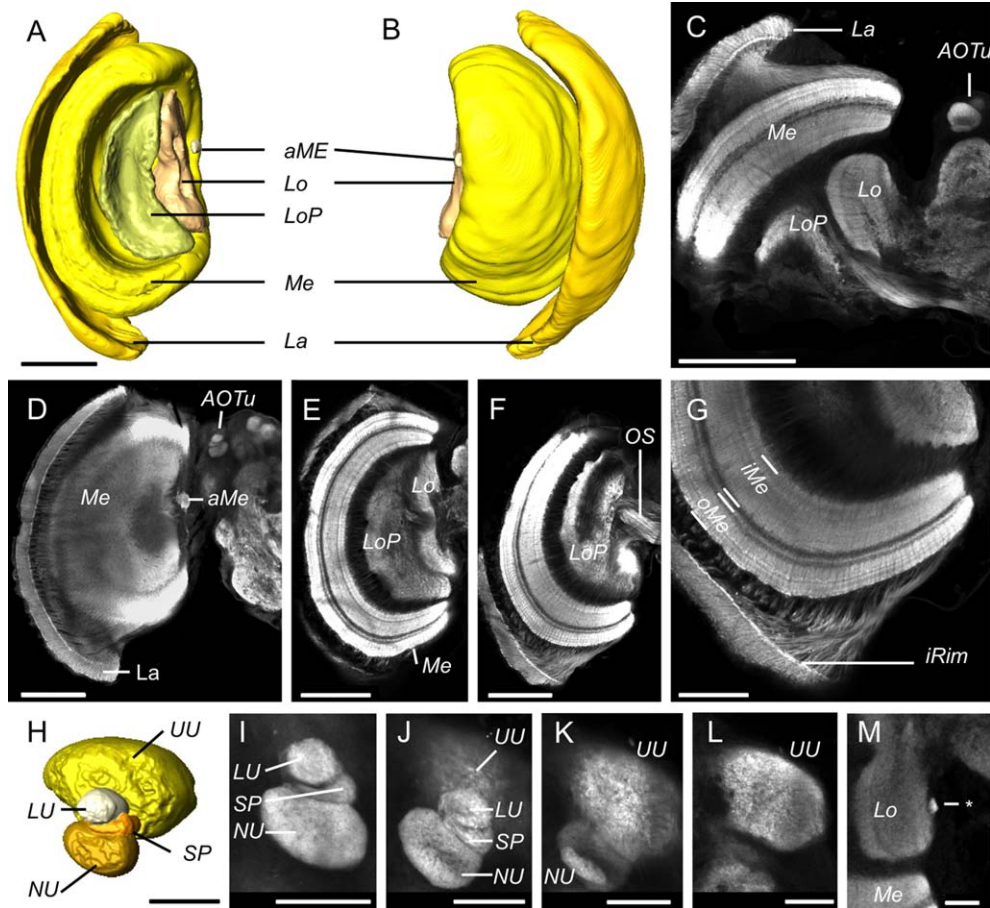


Figure 4. Anatomy of the visual neuropils. **A,B:** Surface reconstructions of the optic lobe neuropils viewed from posterior (A) and anterior (B). They comprise the lamina (La), the medulla (Me), and accessory medulla (aMe), the lobula (Lo), and the lobula plate (LoP). **C–G:** Synapsin immunofluorescence in single confocal sections of the optic lobe. **C:** A horizontal section showing all four major optic lobe neuropils (La, Me, Lo, LoP) together with the anterior optic tubercle (AOTu) in the midbrain. **D–F:** Frontal sections at increasing depths from anterior to posterior, beginning at a plane tangential through the lamina (La in D) and reaching the optic stalk (OS in F). **G:** The inner rim (iRim) of the lamina is a thin layer on its inner surface that is defined by intense synapsin immunofluorescence; it is also visible in C,D,F. Synapsin immunostaining also reveals the laminated structure of the medulla with two main subdivisions, the outer and inner medulla (oMe, iMe). **H:** Surface reconstruction of the AOTu from an oblique anterior view, showing the four component neuropils: the upper unit (UU), lower unit (LU), strap (SP), and the nodular unit (NU). **I–L:** Synapsin immunofluorescence in the AOTu in frontal confocal sections at increasing depths from anterior (I) to posterior (L). **M:** A small neuropil (asterisk) positioned at the medial margin of the lobula which may be homologous to the *D. plexippus* optic glomerular complex. Scale bars = 200 μm in A–F; 100 μm in G; 50 μm in H–M.

the calyx lacks subdivision into an outer, inner, central, and basal zones. Instead, the calyx has a relatively simple structure, a fused double-calyx (Fig. 5F,H,I) more reminiscent of that seen in moths (Pearson, 1971; Homberg et al., 1988; Sjöholm et al., 2005; El Jundi et al., 2009b; Fukushima and Kanzaki, 2009; Kvello et al., 2009). To a certain extent this is also the case for the mushroom body lobes. The vertical and medial lobe systems are more distinct from one another than they are in *D. plexippus* (Heinze and Reppert, 2012), and within the vertical lobe system it is possible to identify the α -lobe and γ -lobe (Fig. 5A). The vertical lobes project dorsoposteriorly towards the upper surface of the brain, visible as a protruding bulge (Fig. 5C).

In the medial lobe the boundaries between the components are less well defined, but they are not fully fused into a globular mass as in *D. plexippus* (Heinze and Reppert, 2012), although identifying further subdivisions homologous to those observed in moths (Rø et al., 2007) is difficult (Fig. 5J,K).

As in other Lepidoptera, the peduncle emerges from a fusion of two tracts of Kenyon cell axons within the fused double-calyx (Fig. 2F,G) and spans the depth of the midbrain to connect with the lobes. The boundary between the peduncle and the lobes is not well defined. A Y-tract is also present, running dorsal and parallel to the peduncle, between the mushroom body lobe and the anterior boundary of the calyx (Y-tract in Fig. 5).

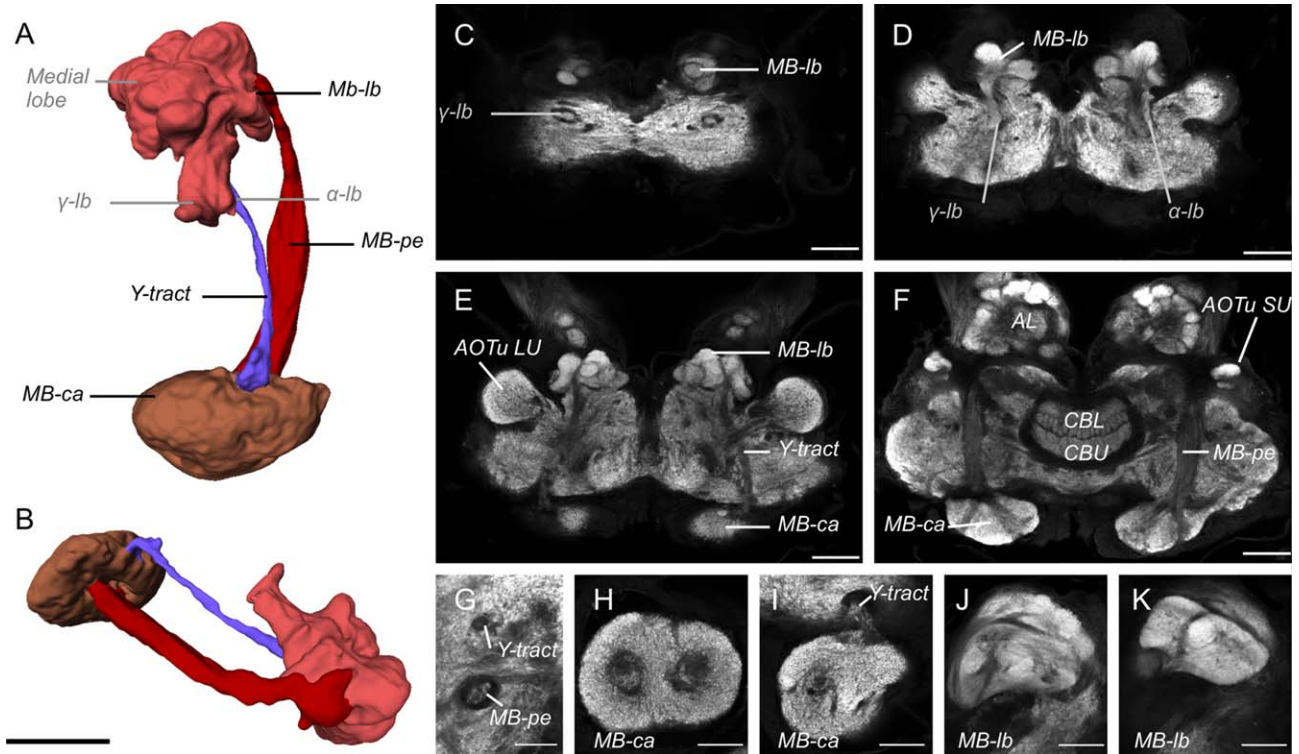


Figure 5. Anatomy of the mushroom body. **A,B:** Surface reconstruction of the mushroom body from the dorsal (A) and lateral (B) view. **C–F:** Synapsin immunofluorescence in horizontal confocal sections through the midbrain at increasing depths from dorsal towards ventral. The very dorsal (tangential) plane C shows the tips of the medial lobe (MB-lb) and of the γ -lobe (γ -lb). D: The main components of the lobes: the α -lb, γ -lb, and the compartmentalized medial lobe (MB-lb). E: The Y-tract runs from the calyx (MB-ca) anteriorly to the lobes (MB-lb). F: Further ventral and level with the upper and lower units of the central body (CBL, CBU), the peduncles (Pe) provide the main connection between MB-ca and MB-lb. **G–K:** Details of mushroom body architecture as revealed by synapsin immunofluorescence in confocal sections. G: Frontal section showing the separate profiles of the Y-tract and pedunculus (MB-pe) in the central mid-brain; dorsal is up. H,I: Frontal sections through the calyx (Mb-ca). H: Each MB-ca consists of two fused calycal neuropils, which lack any obvious internal zonation. I: Emergence of the Y-tract at the anterodorsal boundary of MB-ca. J,K: Morphology of the partially merged dorsal lobe of the MB. Scale bars = 100 μ m in A–F; 50 μ m in G–K.

Interestingly, in *D. plexippus* the Y-tract appears to innervate exclusively the inner zone of the calyx (Heinze and Reppert, 2012), suggesting that this structure may be homologous to the entire un-zonated calyx of *G. zavaleta* and thus represents the ancestral base around which the outer and basal zones have formed as additional derived structures.

The presence of a Y-tract is thought to indicate the presence of Kenyon cells functioning as class III neurons by receiving mechanosensory and gustatory information through the tritocerebral tract (Farris, 2005). In true class III Kenyon cells, the dendrites typically form a distinct accessory calyx. However, no accessory calyx is observed in *G. zavaleta*, unlike in *Pieris brassicae* (Ali, 1974) and *D. plexippus* (Heinze and Reppert, 2012), where it occurs as a distinct neuropil to the anterior of the main calyx. This suggests that the adult brain of *G. zavaleta* may lack true class III cells. They may still have a transient developmental role in establishing circuitry

with the tritocerebral tract before transferring this function to a subpopulation of the class I Kenyon cells and dying (Farris et al., 2004; Farris, 2005). Alternatively, the class III cells of *G. zavaleta* might survive but their dendrites may be integrated into the main calyx.

Central complex

The final major group of neuropils considered here form the central complex (Fig. 6), a multimodal integration center implicated in a range of functions including spatial representation of visual cues, spatial visual memory, and directional control of locomotor behaviors (Pfeiffer and Homberg, 2014). The central complex comprises the central body (CB in Fig. 1E,I) that in turn is composed of an upper division (CBU in Fig. 6A–D), a lower division (CBL in Fig. 6A–D), and the anteriorly associated paired noduli (No in Fig. 6B,H); the protocerebral bridge (PB in Figs. 1E, 6E,F) and the posterior optic tubercle (POTu in Fig. 6E,G). All of these neuropils are

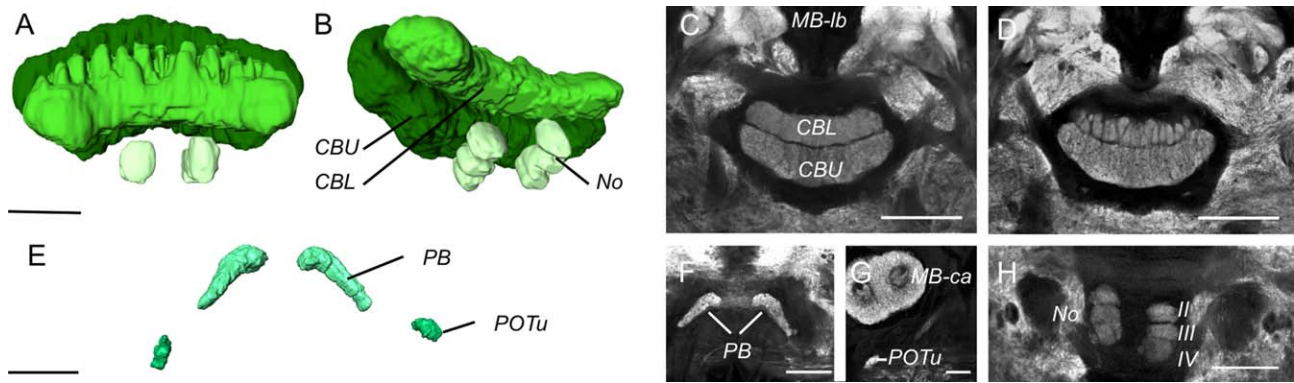


Figure 6. Anatomy of the central complex. **A,B:** Surface reconstruction of the central body from an anterior (A) and oblique anteroventral (B) view, showing the upper and lower subunit of the central body (CBU, CBL) and the three compartments of the noduli (No). **C,D:** Synapsin immunofluorescence in horizontal confocal sections showing the structure of the upper and lower CB (C) and the foliated dorsal surface of the lower CB (D). **E:** Surface reconstruction of the protocerebral bridge (PB) and posterior optic tubercles (POTu) from an oblique posterior view. **F,G:** Synapsin-immunofluorescence in frontal confocal sections showing the PB (F), and the POTu ventral to the MB-ca (G). **H:** The noduli (No) in a horizontal confocal section ventral to the CB showing three discrete compartments homologous to compartments II–IV in *D. plexippus* (Heinze and Reppert, 2012); the intensely stained compartment I, which partially encircles subcompartment II in *D. plexippus* was not clearly visible. Scale bars = 50 μm in A; 100 μm in C–F; 50 μm in G–H.

clearly visible in *G. zavaleta* (Fig. 6). The lateral accessory lobes (LAL), situated at the ventral boundary of the antennal lobes, are also functionally linked to the CB but we refrained from quantifying the size of the LAL due to its poorly defined posterior boundaries. Although the LAL is well stained, we were unable to identify within it any clear anterior lobelet with a microglomerular appearance as observed in *D. plexippus* (Heinze and Reppert, 2012). The general morphology and layout of the remaining central complex is otherwise conserved between *G. zavaleta* and *D. plexippus*, although in the current analysis we did not explore the finer-scale morphology of the central body to confirm the conservation of CB layers. One notable difference is the highly foliated structure of the dorsal surface of the lower CB in *G. zavaleta* (Fig. 5A,D). Although the POTu were easily identifiable they were found to be one of the more variable structures in both volume (Table 1) and shape.

Divergence in brain structure across Lepidoptera

The brain of *G. zavaleta* has a number of features that appear to be intermediate between those observed in moths and *D. plexippus*. We collated comparable datasets for two night-flying moths, *H. virescens* (Kvella et al., 2009) and *M. sexta* (El Jundi et al., 2009b), and a second diurnal butterfly, *D. plexippus* (Heinze and Reppert, 2012), to further explore these differences (Table 3). As a percentage of the total neuropil volume, *G. zavaleta* is intermediate between *D. plexippus* and

the moths for all major sensory neuropil, with larger antennal lobes and smaller visual neuropil than *D. plexippus* (Table 3). To remove the dominant effect of the large optic lobe neuropil we repeated the comparison focusing on the relative size of structures within the midbrain. Again, in terms of percentage volume, the antennal lobes and the mushroom body of *G. zavaleta* are much closer to the moths than *D. plexippus* (Table 3). This pattern is borne out in a multivariate principal component (PC) analysis measuring relative size as deviation from interspecific allometric relationships with total brain size (Fig. 7). The four species are clearly separated along two PCs. Considering all neuropil, including the optic lobes, PC1 explains 77.82% of the variance and is most heavily loaded by the antennal lobe and medulla, while PC2 explains 21.16% of the variance and is most heavily loaded by the mushroom body calyx, peduncle and lobes (Fig. 7A, Table 4). Considering only the midbrain PC1 explains 86.83% of the variance and is most heavily loaded by the mushroom body calyx, peduncle and lobes, and AOTu, while PC2 explains 11.34% of the variance and is most heavily loaded by the central body and AOTu (Fig. 7B, Table 4). Similar results are obtained from a PC analysis with percentage volumes (Table 4).

DISCUSSION

We have described the anatomical layout and size of the major neuropils in the brain of *Godyris zavaleta*, a diurnal butterfly with a heightened dependence on

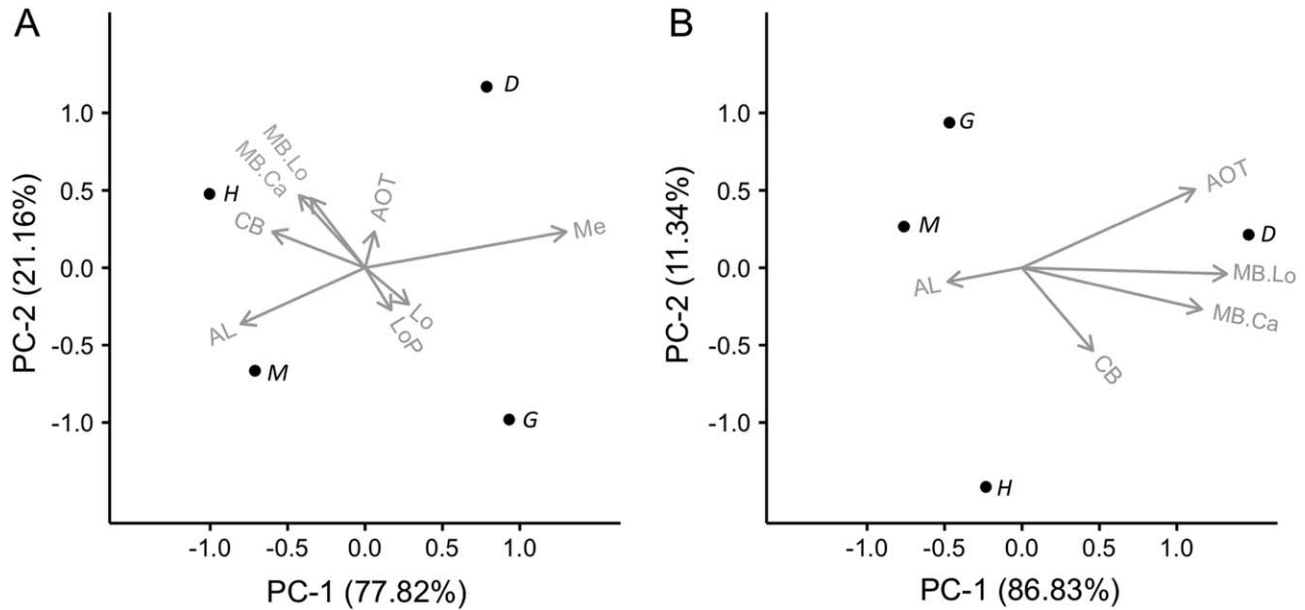


Figure 7. Principal component (PC) biplots of the relative size of major brain structures in four Lepidoptera. **A:** PC analysis of all neuropil. **B:** PC analysis excluding the optic lobe neuropil. In both cases the PC analysis was performed using residuals from a phylogenetically controlled regression between each neuropil and the rest of the total neuropil/total midbrain. Analysis using volumes expressed as percentages results in similar conclusions (Table 4). The biplots show each species as a data point labeled with the first letter of the genus name (D = *Danaus*, G = *Godyris*, H = *Heliiothis*, M = *Manduca*); vectors lengths are proportional to the variance of that variable/neuropil.

olfactory information. The antennal lobes of *G. zavaleta* have a unique morphology compared to other butterflies examined so far (Rospars, 1983; Heinze and Reppert, 2012; Carlsson et al., 2013), with a distinct cluster of four enlarged glomeruli, of which two are sexually dimorphic. Based on their size, location, and the

fibrous appearance of their internal structure, we tentatively label these four glomeruli as a macroglomerular complex analogous to the MGCs present in a wide variety of moths (Bretschneider, 1924; Rospars, 1983; Berg et al., 2002; Huetteroth and Schachtner, 2005; Masante-Roca et al., 2005; Skiri et al., 2005; El Jundi et al., 2009b; Kazawa et al., 2009; Varela et al., 2009). Through an interspecific analysis within Lepidoptera, we further show the adaptation to greater olfactory dependence extends to the major sensory neuropils, with the relative size of the visual and olfactory neuropil of *G. zavaleta* being intermediate between night-flying moths and the diurnal monarch butterfly. In the following discussion we explore the selection pressures that may have favored these adaptations, the potential relationship of the *G. zavaleta* MGC to the MGC in moths and other insects, and the strength of constraints that may limit the effect of selection on brain composition.

Ecological relevance of sexual dimorphism in the antennal lobe

To our knowledge, a morphologically distinct and sexually dimorphic MGC has not been described in any of the butterflies previously examined (*Pieris brassicae*, Rospars, 1983; *Danaus plexippus*, Heinze and Reppert, 2012; *Polygonia c-album* and *Aglais urticae*, Carlsson et al., 2013). Physiological studies will be necessary to

TABLE 4.

Loadings on Principal Components Analysis of Relative Size of Brain Components Across Four Lepidoptera

Neuropil	Loadings			
	Residuals		Percentages	
	PC1	PC2	PC1	PC2
a) Midbrain only				
Antennal lobe	-0.219	0.114	-0.753	0.649
Central body	0.209	0.678	0.053	0.014
Calyx	0.531	0.339	0.504	0.539
Peduncle and lobes	0.605	0.050	0.385	0.530
AOTu	0.511	-0.640	0.168	0.077
b) Whole neuropil				
Antennal lobe	0.455	-0.395	0.080	0.748
Central body	0.339	0.253	0.017	-0.063
Calyx	0.242	0.509	0.021	-0.131
Peduncle and lobes	0.198	0.489	0.002	-0.018
AOTu	-0.034	0.253	-0.002	-0.034
Medulla	-0.737	0.254	-0.994	0.014
Lobula	-0.160	-0.257	-0.060	0.400
Lobula plate	-0.096	-0.297	-0.035	0.507

confirm that the MGC of *G. zavaleta* has the predicted role in pheromone detection. For the time being, two hypotheses can be made regarding its ecological relevance. First, detecting pheromonal cues used in mating and/or territorial defense. Second, detecting allelochemicals from plants that provide males with the PA precursors from which they synthesize their pheromones.

Male ithomiines utilize PA-derived pheromones in male–male territorial interactions and male–female courtship (Gilbert, 1969; Pliske, 1975a; Edgar et al., 1976). The specially adapted hind-wing hair-pencils help distribute these pheromones during flight. In the absence of females, many species embark on short, circling flights that fill the airspace with pheromone secretions (Pliske, 1975a; Drummond, 1976). This suggests that the signal is distributed over larger spatial scales than typical for butterflies. Most species of Danainae also utilize PA-derived pheromones in sexual communication (Pliske et al., 1976; Trigo and Motta, 1990; Honda et al., 2006). Danainae have hair-pencils located at the tip of the abdomen that are displayed during courtship and persistently brought into contact with the hind-wing, to aid dissemination of chemical secretions (Müller, 1879; Boppré et al., 1978; Brower and Jones, 2009). Although Danainae may utilize chemical communication on smaller spatial scales than Ithomiinae, it remains possible that the lack of sexually dimorphic glomeruli in *D. plexippus* is not representative of all Danainae. In the closely related *D. gilippus*, the experimental removal of hair-pencils substantially reduces courtship success (Myers and Brower, 1969) whereas in *D. plexippus*, which has smaller hair pencils than most Danainae, it has no observable effect on reproduction (Pliske, 1975b). Instead, *D. plexippus* matings often occur through "aerial take downs" where males grasp the female in mid-air, causing them to fall to the ground where the male attempts to mate (Pliske, 1975b). This behavior is also observed in the ithomiine genus *Methona* (Pliske, 1975a). Comparisons across Danainae and Ithomiinae with contrasting mating behaviors may provide independent tests of whether sexually dimorphic glomeruli are associated with the dominance of hair-pencil mediated pheromone signaling in mating behavior (Gilbert, 1969; Pliske, 1975a; Drummond, 1976; Haber, 1978).

An alternative explanation may be that the sexually dimorphic glomeruli of *G. zavaleta* are specialized to detect odors emanating from plants used to obtain PAs for pheromone synthesis and chemical protection. In most ithomiine species, males, but not females, are strongly attracted to *Heliotropium* bait traps and use olfaction to locate these resources (Pliske et al., 1976). In the wild these resources may be transitory, with

decaying *Heliotropium* losing its attractive properties after 2 weeks in wet conditions (Pliske et al., 1976). As the estimated average lifespan across ithomiines is ~10 weeks and potentially up to 25 weeks (Drummond, 1976), enhancing foraging efficiency with olfactory adaptations may be more efficient than learning the location of transient resources. It is conceivable that selection for increased foraging efficiency targeted the antennal lobe in a sex-specific manner. Although less common, macroglomeruli associated with nonsexual pheromones are found in some taxa (Galizia and Rössler, 2010; Hansson and Stensmyr, 2011), most notably in leaf cutter ants (*Atta vollenweideri*, *Atta sexdens*) where the single macroglomerulus processes trail-pheromones (Kleineidam et al., 2005), and in *Drosophila sechellia*, where large glomeruli are involved in specialization to a single food source (Dekker et al., 2006).

Evolution of sexual dimorphism in the antennal lobe

Sexually dimorphic MGCs, or single macroglomeruli, are sporadically found in phylogenetically distant insect clades, and are generally considered the result of convergent evolution (Schachtner et al., 2005; Hansson and Stensmyr, 2011). A possible homology of MGCs among more closely related clades, such as the Lepidoptera, has received insufficient discussion, given its importance in interpreting patterns of neural evolution. As pointed out by Scotland (2010), "... every hypothesis of homology requires a conditional or specifying phrase; homologous as what?" Thus, at any given phylogenetic level, one may ask whether MGCs are homologous as *structures*, that is, linked through unbroken phylogenetic presence to a set of glomeruli in the last common ancestor. Whether structurally homologous glomeruli have had an unbroken *functional* history in pheromone detection, and whether this function was always associated with male-specific *enlargement* are separate questions, as enlargements could occur in parallel in structurally homologous glomeruli. Given the phylogenetic position of the butterflies examined thus far (Freitas and Brown, 2004; Wahlberg, 2006; Regier et al., 2013) it seems most likely that the male-specific enlargement of particular glomeruli into an MGC is a secondarily derived trait of *G. zavaleta* among butterflies, and an example of convergence at the level of the Lepidoptera. Whether the putative MGC in *G. zavaleta* is homologous to the MGCs in moths at the level of "structural correspondence" is less clear. Indeed, the homology of the MGC among moths is not established. The number of glomerular units that comprise the MGC in moths varies between species, partly but not wholly dependent on the number of chemical components in the species' pheromone blend (Hansson

et al., 1991; Todd et al., 1995; Berg et al., 1998). Structural homology may therefore be limited to a core set of glomeruli, or a single glomerulus, and the associated neural circuitry, around which the MGC evolves in a taxa-specific manner.

That male-specific MGCs can evolve rapidly and independently even at the family and genus level is witnessed by the report that an MGC has evolved independently multiple times in the two *Drosophilid* genera, *Drosophila* and *Scaptomyza* (Kondoh et al., 2003). Among Hawaiian species, it is the same two (quite uncontentiously homologous) glomeruli, DA1 and DL3, that have been independently enlarged in males in multiple lineages, a case of parallelism of enlargement of homologous structures. But within *D. melanogaster* specifically, enlargement affects DA1 and VA1v, rather than DL3 (Kondoh et al., 2003). Therefore, even within one genus, structurally nonhomologous glomeruli can show convergent male-specific enlargement. Similarly, five species of bombycid moths share a core set of two sexually dimorphic macroglomeruli, the toroid and cumulus, to which two additional glomeruli have been co-opted into the MGC in *Rondotia* and *Bombyx* (Namiki et al., 2014). By extrapolation, it is possible that all Lepidopteran MGCs contain a structurally homologous core glomerulus (like DA1 within *Drosophilids*), but we currently lack sufficient information to test this hypothesis.

The fundamental problem here lies in the difficulty of identifying corresponding glomeruli across taxa. The consistent positioning of MG(C)s at the root of the antennal nerve may reflect the outcome of a convergent wiring optimization (Rospars, 1983) and is therefore not a suitable homology criterion. One might define homologous glomeruli according to the orthology of their associated olfactory receptors (ORs), on the basis that the gene-regulatory link between OR gene expression and glomeruli formation might couple gains and losses in OR genes to concomitant gains and losses of glomeruli (see below). However, in *Drosophila* OR expression is not required for glomerulus-specific axonal targeting, which is instead controlled by separate mechanisms (Dobritsa et al., 2003; Hummel et al., 2003; Hong and Luo, 2014). It therefore seems conceivable that OR gene expression can be switched out for expression of a nonorthologous OR in a structurally homologous glomerulus. Hence, while gene expression can provide useful information, it is not suitable for establishing structural homology.

Establishing homology between glomeruli is of clear importance, as it permits the identification of independent gains and losses of an MGC. This would provide further insights into how olfactory information is coded in different species, and how labile the underlying neural

networks are. For example, chemical communication is known to play a significant role in butterfly biology (Scott, 1973; Andersson et al., 2007; Costanzo and Monteiro, 2007) and species that lack an MGC presumably retain the ability to detect pheromones. In moths, the sex pheromone response is thought to be restricted to the MGC, while plant odors are processed in the ordinary glomeruli, creating two parallel olfactory systems (Galizia et al., 2000; Hansson and Anton, 2000; Galizia and Rössler, 2010), although crosstalk between the pheromone and ordinary glomeruli subsystems may occur (Trona et al., 2010, 2013). Whether the loss of an MGC merely reflects a decrease in the volume of pheromone-associated glomeruli while the distinction between two parallel olfactory systems is maintained, or whether there is a concomitant wider integration of this function across ordinary glomeruli, is not yet clear. Exclusive pheromone detection by ordinary glomeruli is observed in some honeybee castes but this may be a special case linked to chemical similarity between pheromones and other environmental odors (Sandoz et al., 2007).

Sensory adaptations in Lepidoptera

Beyond the sexually dimorphic glomeruli there is a clear signal of sensory adaptation in the major neuropils. Consistent with the expectation that visual information is more important for diurnal Lepidoptera, while olfactory information plays a greater role in night-flying species (Hambäck et al., 2007), a PCA largely separates moths from butterflies along an axis representing the size of the antennal lobes and the largest visual neuropil, the medulla. More subtle effects are also apparent, with the crepuscular *M. sexta*, which has relatively high visual acuity for a moth (Theobald et al., 2010), having a proportionately larger medulla than *H. virescens*, which is predominantly nocturnal (Hayes, 1991; Topper, 2009), while the size of the *G. zavaleta* medulla and antennal lobe are intermediate between the moths and *D. plexippus*.

The observed interspecific variation in antennal lobe size contrasts with the relative constancy of glomerular number. Across Lepidoptera the total number of glomeruli found in each antennal lobe is between 60 and 70 (Boeckh and Boeckh, 1979; Rospars, 1983; Berg et al., 2002; Huetteroth and Schachtner, 2005; Masante-Roca et al., 2005; Skiri et al., 2005; Kazawa et al., 2009; Carlsson et al., 2013) with the exception of the oligophagous moth genus *Cydia*, which has only ~50 (Varela et al., 2009; Couton et al., 2009; Trona et al., 2010). Evidently, variation in antennal lobe size must be caused by variation in the average size of the glomeruli and/or changes in the size of the central fibrous neuropil. The former may reflect heightened

sensitivity as the glomeruli receive projections from more olfactory sensory neurons, while the latter may reflect changes in the number and structure of local interneurons (and possibly of projection interneurons). This would result in altered processing of combinatorial excitation, perhaps enhancing odor discrimination.

The relatively constant number of glomeruli further contrasts with the apparent high evolutionary turnover of OR genes in Lepidoptera (Zhan et al., 2011; Dasmahapatra et al., 2012). Although drift may also have a role (Gardiner et al., 2008), duplicated OR genes likely reflect functional changes in olfaction favored by changing ecological conditions (Hansson and Stensmyr, 2011). In *Drosophila*, closely related ORs project to adjacent glomeruli (Couto et al., 2005; Silbering et al., 2011), suggesting new glomeruli may often evolve through fission events (Ramdya and Benton, 2010). This process may be genetically linked to OR duplication, as cis-regulatory regions regulating OR expression are also found upstream of genes controlling olfactory sensory neuron axon growth (Ray et al., 2008). Hence, ORs and their associated glomeruli may form readily adaptable, interchangeable modules that can be readily acquired and discarded through gain and loss of OR genes (Cande et al., 2013). This in turn implies that the roughly constant number of glomeruli across Lepidoptera masks a high evolutionary turnover of OR genes, meaning only few glomeruli may be linked to homologous ORs across species. This scenario, however, is not readily reconciled with recent reports that a variety of odors elicit similar antennal lobe excitation maps in two ecologically distinct Nymphalids and three closely related sphingid moths, suggesting conservation of glomerular tuning (Bisch-Knaden et al., 2012; Carlsson et al., 2013). Reconciling these apparently contrasting patterns of divergence at the genomic and anatomical level, and understanding what selection pressures or constraints limit the range of glomerular number in Lepidoptera, may shed much light on the function and evolution of olfactory networks.

Conservation and divergence in neuropil

One of the most debated themes in comparative vertebrate neurobiology is the extent to which genetic and developmental constraints limit the scope of adaptive evolution of brain structure, enforcing a concerted, as opposed to a mosaic, pattern of brain evolution (Finlay and Darlington, 1995; Barton and Harvey, 2000). Our analysis suggests that invertebrate brains can readily respond to changing selection pressures, with the gain and loss of distinct structures, or subcompartmentalization of existing neuropil, occurring in a lineage-specific manner, often without any clear correlative change in

other structures. Within Lepidoptera, species vary markedly not only in the relative volume of different neuropils, as discussed above, but also in the presence or absence of some traits such as the optic glomeruli, the AOTu strap, and the zonation of the mushroom body calyx. Indeed, some traits diverge in a manner that does not reflect phylogenetic relatedness, or any obvious ecological variable. A notable example is the presence of an accessory calyx in the mushroom body of *P. brassicae* (Ali, 1974) and *D. plexippus* (Heinze and Reppert, 2012), but not of *G. zavaleta*. Among moths, an accessory calyx is present in *M. sexta* (Homberg et al., 1988), but not in *H. virescens* (Kvellido et al., 2009; Løfaldli et al., 2010) or several other species (Bretschneider, 1924; Pearson, 1971). This repeated gain and loss of the accessory calyx is common across invertebrates (Farris, 2005) but the functional significance is unclear.

A final notable aspect of Lepidopteran brain evolution is the lack of apparent coevolution between the antennal lobes and the mushroom body calyces. The calyces are one of only two neuropils that receive direct innervation from the axons of antennal lobe projection neurons, the other being the lateral protocerebrum. It may therefore be reasonable to expect a positive coevolutionary relationship between antennal lobe size and the mushroom body calyx (Strausfeld and Li, 1999; Farris, 2005). Indeed, insects that show an extreme evolutionary reduction or total loss of their antennal lobes also typically lack calyces (Strausfeld et al., 1998; Farris and Roberts, 2005). However, the present analysis within Lepidoptera provides little evidence for graded concomitant changes in antennal lobe and calyx size. In some instances, the explanation may be that substantial portions of the calyx are given over to non-olfactory tasks (Sjöholm et al., 2005; Heinze and Reppert, 2012). We note, however, that a decoupling of AL and MB calyx size does not in itself imply that part of the calyx has assumed nonolfactory functions: it may instead reflect the distinct computational roles of the AL and MB in olfaction (Laurent et al., 1998; Laurent, 2002). For example, selection for increased odor sensitivity may drive an increase in the number of receptor neurons and thus result in bigger glomeruli, but would not require more projection neurons or any changes in the calyx. The patterns seen among Lepidoptera indicate that, apart from the extreme case of anosmic insects, the forces driving coevolution of AL and MB size are only moderate, and refutes the naïve expectation that reliance on olfactory information will drive the expansion of both structures. Deciphering whether this mosaic pattern of change is a common feature of invertebrate brain evolution will

require further comparative data, but proportional differences in brain structure have been reported for a number of taxa (Ott and Rogers, 2010; O'Donnell et al., 2011, 2013).

CONCLUSIONS AND FUTURE PROSPECTS

In this study we present multiple lines of evidence that ecology-specific behavioral selection pressures shape the composition of invertebrate brains. In the butterfly *G. zavaleta*, heightened reliance on olfaction apparently drove the independent evolution of a group of specialized olfactory glomeruli into a prominent MGC with a putative function analogous to the pheromone-sensing MGC in moths. Combined with recent genomic (Zhan et al., 2011; Dasmahapatra et al., 2012) and neurophysiological and ecological evidence (Andersson et al., 2007; Costanzo and Monteiro, 2007; Carlsson et al., 2013) this reinforces the importance of olfaction in some diurnal butterflies, a group traditionally perceived as relying primarily on visual information. To the extent that brain composition reflects adaptations rather than developmental or functional constraints, the relative sizes of brain structures should differ according to their importance to an organism's behavior (Barton et al., 1995; Gronenberg and Hölldobler, 1999; De Winter and Oxnard, 2001; El Jundi et al., 2009a,b; Wei et al., 2010; Heinze and Reppert, 2012). We found that the size of the sensory neuropil can be directly related to a species' diel pattern of activity and habitat preference across four species of Lepidoptera. This is true both when comparing two moths with two butterflies, and when comparing a nocturnal and a crepuscular moth, or a more visually and a more olfactorily driven butterfly. Our results also uncover a strong signature of a mosaic pattern of brain structure evolution. Whatever developmental and functional constraints may operate in invertebrate brains, they clearly permit adaptive (sensu mosaic) evolution of brain structure with expansions in certain neuropils occurring without concomitant expansion in all functionally related structures. These results suggest future comparative studies across many more species may be useful in illuminating the ecological and behavioral relevance of neuropil size and structure, and the significance of connections between neuropils.

ACKNOWLEDGMENTS

S.H.M. thanks Álvaro Barragán, Emilia Moreno, Pablo Jarrín, and David Lasso from the Estación Científica Yasuní and Pontificia Universidad Católica del Ecuador, and María Arévalo from the Parque Nacional Yasuní, Ministerio Del Ambiente for assistance with collection and exportation permits, and Francisco Ramírez Castro for excellent

assistance in the field. S.H.M. also thanks Chris Jiggins, Richard Merrill, Keith Willmott, Marianne Elias, and Judith Mank's research group at UCL for helpful advice and feedback, Rémi Blanc for advice on merging and labeling confocal images, Stanley Heinze for providing the volumetric data for *D. plexippus* and additional advice on data processing, and Daniel Ciantar and Tim Robson at the UCL Imaging Facility for help with confocal microscopy.

CONFLICT OF INTEREST

The authors declare no conflict of interest.

ROLE OF AUTHORS

Both authors read and approved the final article. Study concept, design and preliminary experiments: S.H.M., S.R.O. Fieldwork, acquisition of data, analysis, interpretation, and initial article draft: S.H.M. Final interpretation and drafting: S.H.M., S.R.O.

LITERATURE CITED

- Ali FA. 1974. Structure and metamorphosis of the brain and suboesophageal ganglion of *Pieris brassicae* (L.) (Lepidoptera: Pieridae). *Trans R Entomol Soc Lond* 125:363–412.
- Andersson S, Dobson HEM. 2003. Behavioral foraging responses by the butterfly *Heliconius melpomene* to *Lantana camara* floral scent. *J Chem Ecol* 29:2303–2318.
- Andersson J, Borg-Karlson A-K, Vongvanich N, Wiklund C. 2007. Male sex pheromone release and female mate choice in a butterfly. *J Exp Biol* 210:964–970.
- Barton RA, Harvey PH. 2000. Mosaic evolution of brain structure in mammals. *Nature* 405:1055–1058.
- Barton RA, Purvis A, Harvey PH. 1995. Evolutionary radiation of visual and olfactory brain systems in primates, bats and insectivores. *Philos Trans R Soc Lond B Biol Sci* 348:381–392.
- Bates HW. 1862. XXXII. Contributions to an insect fauna of the Amazon Valley. Lepidoptera: Heliconidae. *Trans Linn Soc Lond* 23:495–566.
- Beccaloni GW. 1997. Ecology, natural history and behaviour of ithomiine butterflies and their mimics in Ecuador (Lepidoptera: Nymphalidae: Ithomiinae). *Trop Lepid* 8:102–124.
- Berg BG, Almaas TJ, Bjaalie JG. 1998. The macroglomerular complex of the antennal lobe in the tobacco budworm moth *Heliothis virescens*: specified subdivision in four compartments according to information about biologically significant compounds. *J Comp Physiol A* 183:669–682.
- Berg BG, Galizia CG, Brandt R, Mustaparta H. 2002. Digital atlases of the antennal lobe in two species of tobacco budworm moths, the Oriental *Helicoverpa assulta* (male) and the American *Heliothis virescens* (male and female). *J Comp Neurol* 446:123–134.
- Bisch-Knaden S, Carlsson MA, Sugimoto Y, Schubert M, Mißbach C, Sachse S, Hansson BS. 2012. Olfactory coding in five moth species from two families. *J Exp Biol* 215:1542–1551.
- Boeckh J, Boeckh V. 1979. Threshold and odor specificity of pheromone-sensitive neurons in the deutocerebrum of *Antheraea pernyi* and *A. polyphemus* (Saturniidae). *J Comp Physiol A* 132:235–242.

- Boppré M, Petty RL, Schneider D, Meinwald J. 1978. Behaviorally mediated contacts between scent organs: another prerequisite for pheromone production in *Danaus chrysipus* males (Lepidoptera). *J Comp Physiol A* 126:97–103.
- Brandt R, Rohlfing T, Rybak J, Krofczik S, Maye A, Westerhoff M, Hege H-C, Menzel R. 2005. Three-dimensional average-shape atlas of the honeybee brain and its applications. *J Comp Neurol* 492:1–19.
- Bretschneider OH. 1924. Über die Gehirne des Eichenspinners und des Seidenspinners (*Lasiocampa quercus* L. und *Bombyx mori* L.). *Jena Z Naturw* 60:563–570.
- Briscoe AD, Macias-Muñoz A, Kozak KM, Walters JR, Yuan F, Jamie GA, Martin SH, Dasmahapatra KK, Ferguson LC, Mallet J, Jacquin-Joly E, Jiggins CD. 2013. Female behaviour drives expression and evolution of gustatory receptors in butterflies. *PLoS Genet* 9:e1003620.
- Brower LP, Jones MA. 2009. Precourtship interaction of wing and abdominal sex glands in male *Danaus* butterflies. *Proc R Entomol Soc Lond Ser A Gen Entomol* 40:147–151.
- Brower LP, Brower JVZ, Collins CT. 1963. Experimental studies of mimicry: Relative palatability and Müllerian mimicry among Neotropical butterflies of the subfamily Heliconiinae. *Zoologica* 48:65–83.
- Brown KS Jr. 1984. Chemical ecology of dehydropyrrolizidine alkaloids in adult Ithomiinae (Lepidoptera: Nymphalidae). *Revisita Bras Biol* 44:435–460.
- Cande J, Prud'homme B, Gompel N. 2013. Smells like evolution: the role of chemoreceptor evolution in behavioral change. *Curr Opin Neurobiol* 23:152–158.
- Carlsson MA, Bisch-Knaden S, Schäpers A, Mozuraitis R, Hansson BS, Janz N. 2011. Odour maps in the brain of butterflies with divergent host-plant preferences. *PLoS One* 6:e24025.
- Carlsson MA, Schäpers A, Nässel DR, Janz N. 2013. Organization of the olfactory system of nymphalidae butterflies. *Chem Senses* 38:355–367.
- Costanzo K, Monteiro A. 2007. The use of chemical and visual cues in female choice in the butterfly *Bicyclus anynana*. *Proc Biol Sci* 274:845–851.
- Couto A, Alenius M, Dickson BJ. 2005. Molecular, anatomical, and functional organization of the *Drosophila* olfactory system. *Curr Biol* 15:1535–1547.
- Couton L, Minoli S, Kiéu K, Anton S, Rospars JP. 2009. Constancy and variability of identified glomeruli in antennal lobes: computational approach in *Spodoptera littoralis*. *Cell Tissue Res* 337:491–511.
- Dasmahapatra KK, Walters JR, Briscoe AD, Davey JW, Whibley A, Nadeau NJ, Zimin AV., Hughes DST, Ferguson LC, Martin SH, Salazar C, Lewis JJ, Adler S, Ahn S-J, Baker DA, Baxter SW, Chamberlain NL, Chauhan R, Counterman BA, Dalmay T, Gilbert LE, Gordon K, Heckel DG, Hines HM, Hoff KJ, Holland PWH, Jacquin-Joly E, Jiggins FM, Jones RT, Kapan DD, Kersey P, Lamas G, Lawson D, Mapleson D, Maroja LS, Martin A, Moxon S, Palmer WJ, Papa R, Papanicolaou A, Pauchet Y, Ray DA, Rosser N, Salzberg SL, Supple MA, Surridge A, Tenger-Trolander A, Vogel H, Wilkinson PA, Wilson D, Yorke JA, Yuan F, Balmuth AL, Eland C, Gharbi K, Thomson M, Gibbs RA, Han Y, Jayaseelan JC, Kovar C, Mathew T, Muzny DM, Ogeri F, Pu L-L, Qu J, Thornton RL, Worley KC, Wu Y-Q, Linares M, Blaxter ML, French-Constant RH, Joron M, Kronforst MR, Mullen SP, Reed RD, Scherer SE, Richards S, Mallet J, Owen McMillan W, Jiggins CD. 2012. Butterfly genome reveals promiscuous exchange of mimicry adaptations among species. *Nature* 487:94–98.
- De Winter W, Oxnard CE. 2001. Evolutionary radiations and convergences in the structural organization of mammalian brains. *Nature* 409:710–714.
- Dekker T, Ibba I, Siju KP, Stensmyr MC, Hansson BS. 2006. Olfactory shifts parallel superspecialism for toxic fruit in *Drosophila melanogaster* sibling, *D. sechellia*. *Curr Biol* 16:101–109.
- Dobritsa AA, Naters WVDG Van, Warr CG, Steinbrecht RA, Carlson JR, Haven N, Vic C. 2003. Integrating the molecular and cellular basis of odor coding in the *Drosophila* antenna. 37:827–841.
- Dreyer D, Vitt H, Dippel S, Goetz B, El Jundi B, Kollmann M, Huetteroth W, Schachtner J. 2010. 3D standard brain of the red flour beetle *Tribolium castaneum*: a tool to study metamorphic development and adult plasticity. *Front Syst Neurosci* 4:3.
- Drummond BA. 1976. Comparative ecology and mimetic relationships of Ithomiine butterflies in Eastern Ecuador. PhD Dissertation, University of Florida.
- Dunbar RIM. 1992. Neocortex size as a constraint on group size in primates. *J Hum Evol* 22:469–493.
- Edgar RC. 2004. MUSCLE: multiple sequence alignment with high accuracy and high throughput. *Nucleic Acids Res* 32:1792–1797.
- Edgar JA, Culvenor CCJ, Pliske TE. 1976. Isolation of a lactone, structurally related to the esterifying acids of pyrrolizidine alkaloids, from the costal fringes of male Ithomiinae. *J Chem Ecol* 2:263–270.
- El Jundi B, Heinze S, Lenschow C, Kurylas A, Rohlfing T, Homberg U. 2009a. The locust standard brain: a 3D standard of the central complex as a platform for neural network analysis. *Front Syst Neurosci* 3:21.
- El Jundi B, Huetteroth W, Kurylas AE, Schachtner J. 2009b. Anisometric brain dimorphism revisited: implementation of a volumetric 3D standard brain in *Manduca sexta*. *J Comp Neurol* 517:210–225.
- Elias M, Gompert Z, Jiggins C, Willmott K. 2008. Mutualistic interactions drive ecological niche convergence in a diverse butterfly community. *PLoS Biol* 6:2642–2649.
- Farris SM. 2005. Evolution of insect mushroom bodies: old clues, new insights. *Arthropod Struct Dev* 34:211–234.
- Farris SM, Roberts NS. 2005. Coevolution of generalist feeding ecologies and gyrencephalic mushroom bodies in insects. *Proc Natl Acad Sci U S A* 102:17394–17399.
- Farris SM, Abrams AI, Strausfeld NJ. 2004. Development and morphology of class II Kenyon cells in the mushroom bodies of the honey bee, *Apis mellifera*. *J Comp Neurol* 474:325–339.
- Felsenstein J. 1985. Phylogenies and the comparative method. *Am Nat* 125:1–15.
- Finlay B, Darlington R. 1995. Linked regularities in the development and evolution of mammalian brains. *Science* 268:1578–1584.
- Freitas AVL, Brown KS. 2004. Phylogeny of the Nymphalidae (Lepidoptera). *Syst Biol* 53:363–383.
- Fukushima R, Kanzaki R. 2009. Modular subdivision of mushroom bodies by Kenyon cells in the silkworm. *J Comp Neurol* 513:315–330.
- Galizia CG, Rössler W. 2010. Parallel olfactory systems in insects: anatomy and function. *Annu Rev Entomol* 55:399–420.
- Gardiner A, Barker D, Butlin RK, Jordan WC, Ritchie MG. 2008. *Drosophila* chemoreceptor gene evolution: selection, specialization and genome size. *Mol Ecol* 17:1648–1657.
- Gilbert LE. 1969. Some aspects of the ecology and community structure of ithomiid butterflies in Costa Rica. In: *Advanced population biology, individual research reports*. July-August, Organisation for Tropical Studies, Ciudad Universitaria, San Jose, Costa Rica. p 69–93.
- Giovanni Galizia C, Sachse S, Mustaparta H. 2000. Calcium responses to pheromones and plant odours in the antennal lobe of the male and female moth *Heliothis virescens*.

- J Comp Physiol A Sens Neural Behav Physiol 186:1049–1063.
- Goyret J, Markwell PM, Raguso RA. 2007. The effect of decoupling olfactory and visual stimuli on the foraging behavior of *Manduca sexta*. J Exp Biol 210:1398–1405.
- Gronenberg W, Hölldobler B. 1999. Morphologic representation of visual and antennal information in the ant brain. J Comp Neurol 412:229–240.
- Haber WA. 1978. Evolutionary ecology of tropical mimetic butterflies (Lepidoptera: Ithomiidae). PhD Dissertation, University of Minnesota, Minneapolis, MN.
- Hambäck PA, Summerville KS, Steffan-Dewenter I, Krauss J, Englund G, Crist TO. 2007. Habitat specialization, body size, and family identity explain lepidopteran density-area relationships in a cross-continental comparison. Proc Natl Acad Sci U S A 104:8368–8373.
- Hansson BS, Anton S. 2000. Function and morphology of the antennal lobe: new developments. Annu Rev Entomol 45: 203–231.
- Hansson BS, Stensmyr MC. 2011. Evolution of insect olfaction. Neuron 72:698–711.
- Hansson BS, Christensen TA, Hildebrand JG. 1991. Functionally distinct subdivisions of the macroglomerular complex in the antennal lobe of the male sphinx moth *Manduca sexta*. J Comp Neurol 312:264–278.
- Harvey PH, Pagel MD. 1998. The comparative method in evolutionary biology. Oxford, UK: Oxford University Press.
- Hayes L. 1991. Dynamics of nocturnal activity of moths in the *Heliothis* complex (Lepidoptera?: Noctuidae) in cotton. J Econ Entomol 84:855–865.
- Healy SD, Rowe C. 2007. A critique of comparative studies of brain size. Proc R Soc B Biol Sci 274:453–464.
- Heinze S, Reppert SM. 2012. Anatomical basis of sun compass navigation I: the general layout of the monarch butterfly brain. J Comp Neurol 520:1599–1628.
- Heinze S, Florman J, Asokaraj S, El Jundi B, Reppert SM. 2013. Anatomical basis of sun compass navigation. II: The neuronal composition of the central complex of the monarch butterfly. J Comp Neurol 521:267–298.
- Hill RI. 2010. Habitat segregation among mimetic ithomiine butterflies (Nymphalidae). Evol Ecol 24:273–285.
- Hofbauer A, Ebel T, Waltenspiel B, Oswald P, Chen YC, Halder P, Biskup S, Lewandowski U, Winkler C, Sickmann A, Buchner S, Buchner E. 2009. The Wuerzburg hybridoma library against *Drosophila* brain. J Neurogenet 23:78–91.
- Homberg U, Montague RA, Hildebrand JG. 1988. Anatomy of antenno-cerebral pathways in the brain of the sphinx moth *Manduca sexta*. Cell Tissue Res 254:255–281.
- Homberg U, Hofer S, Pfeiffer K, Gebhardt S. 2003. Organization and neural connections of the anterior optic tubercle in the brain of the locust, *Schistocerca gregaria*. J Comp Neurol 462:415–430.
- Honda Y, Honda K, Omura H. 2006. Major components in the hairpencil secretion of a butterfly, *Euploea mulciber* (Lepidoptera, Danaidae): their origins and male behavioral responses to pyrrolizidine alkaloids. J Insect Physiol 52: 1043–1053.
- Hong W, Luo L. 2014. Genetic control of wiring specificity in the fly olfactory system. Genetics 196:17–29.
- Huetteroth W, Schachtner J. 2005. Standard three-dimensional glomeruli of the *Manduca sexta* antennal lobe: a tool to study both developmental and adult neuronal plasticity. Cell Tissue Res 319:513–524.
- Hummel T, Vasconcelos ML, Clemens JC, Fishilevich Y, Vosshall LB, Zipursky SL, Angeles L. 2003. Axonal targeting of olfactory receptor neurons in *Drosophila* is controlled by Dscam. Neuron 37:221–231.
- Iwaniuk AN, Dean KM, Nelson JE. 2004. A mosaic pattern characterizes the evolution of the avian brain. Proc Biol Sci 271(Suppl):S148–151.
- Kaye WJ. 2009. XXII. Additions and corrections to my catalogue of the Lepidoptera *Rhopalocera* of Trinidad (1904). Trans R Entomol Soc Lond 61:545–585.
- Kazawa T, Namiki S, Fukushima R, Terada M, Soo K, Kanzaki R. 2009. Constancy and variability of glomerular organization in the antennal lobe of the silkworm. Cell Tissue Res 336:119–136.
- Klagges BR, Heimbeck G, Godenschwege TA, Hofbauer A, Pflugfelder GO, Reifegerste R, Reisch D, Schaupp M, Buchner S, Buchner E. 1996. Invertebrate synapsins: a single gene codes for several isoforms in *Drosophila*. J Neurosci 16:3154–3165.
- Kleineidam CJ, Obermayer M, Halbich W, Rössler W. 2005. A macroglomerulus in the antennal lobe of leaf-cutting ant workers and its possible functional significance. Chem Senses 30:383–392.
- Kondoh Y, Kaneshiro KY, Kimura K, Yamamoto D. 2003. Evolution of sexual dimorphism in the olfactory brain of Hawaiian *Drosophila*. Proc Biol Sci 270:1005–1013.
- Kurylas AE, Rohlfing T, Kroficzek S, Jenett A, Homberg U. 2008. Standardized atlas of the brain of the desert locust, *Schistocerca gregaria*. Cell Tissue Res 333:125–145.
- Kvello P, Løfaldli BB, Rybak J, Menzel R, Mustaparta H. 2009. Digital, Three-dimensional average shaped atlas of the *Heliothis virescens* brain with integrated gustatory and olfactory neurons. Front Syst Neurosci 3:14.
- Labandeira CC, Dilcher DL, Davis DR, Wagner DL. 1994. Ninety-seven million years of angiosperm-insect association: paleobiological insights into the meaning of coevolution. Proc Natl Acad Sci U S A 91:12278–12282.
- Laurent G. 2002. Olfactory network dynamics and the coding of multidimensional signals. Nat Rev Neurosci 3:884–895.
- Laurent G, Macleod K, Stopfer M, Wehr M. 1998. Spatiotemporal structure of olfactory inputs to the mushroom bodies. Learn Mem 5:124–132.
- Løfaldli BB, Kvello P, Mustaparta H. 2010. Integration of the antennal lobe glomeruli and three projection neurons in the standard brain atlas of the moth *Heliothis virescens*. Front Syst Neurosci 4:5.
- Masante-Roca I, Gadenne C, Anton S. 2005. Three-dimensional antennal lobe atlas of male and female moths, *Lobesia botrana* (Lepidoptera: Tortricidae) and glomerular representation of plant volatiles in females. J Exp Biol 208:1147–1159.
- Montgomery SH. 2013. The human frontal lobes: not relatively large but still disproportionately important? A commentary on Barton and Venditti. Brain Behav Evol 82:147–149.
- Müller F. 1879. *Ituna* and *Thyridia*: a remarkable case of mimicry in butterflies. Trans Entomol Soc Lond 20–29.
- Myers J, Brower LP. 1969. A behavioural analysis of the courtship pheromone receptors of the Queen butterfly, *Danaus gilippus berenice*. J Insect Physiol 15:2117–2130.
- Nakagawa T, Sakurai T, Nishioka T, Touhara K. 2005. Insect sex-pheromone signals mediated by specific combinations of olfactory receptors. Science 307:1638–1642.
- Namiki S, Daimon T, Iwatsuki C, Shimada T, Kanzaki R. 2014. Antennal lobe organization and pheromone usage in bombycid moths. Biol Lett 10:20140096.
- O'Donnell S, Clifford M, Molina Y. 2011. Comparative analysis of constraints and caste differences in brain investment among social paper wasps. Proc Natl Acad Sci U S A 108:7107–7112.

- O'Donnell S, Clifford MR, DeLeon S, Papa C, Zahedi N, Bulova SJ. 2013. Brain size and visual environment predict species differences in paper wasp sensory processing brain regions (hymenoptera: vespidae, polistinae). *Brain Behav Evol* 82:177–184.
- Ômura H, Honda K. 2009. Behavioral and electroantennographic responsiveness of adult butterflies of six nymphalid species to food-derived volatiles. *Chemoecology* 19:227–234.
- Ott SR. 2008. Confocal microscopy in large insect brains: zinc-formaldehyde fixation improves synapsin immunostaining and preservation of morphology in whole-mounts. *J Neurosci Methods* 172:220–230.
- Ott SR, Rogers SM. 2010. Gregarious desert locusts have substantially larger brains with altered proportions compared with the solitary phase. *Proc Biol Sci* 277:3087–3096.
- Pagel M. 1999. Inferring the historical patterns of biological evolution. *Nature* 401:877–884.
- Pearson L. 1971. The corpora pedunculata of *Sphinx ligustri* L. and other Lepidoptera: an anatomical study. *Philos Trans R Soc B Biol Sci* 259:477–516.
- Pfeiffer K, Homberg U. 2014. Organization and functional roles of the central complex in the insect brain. *Annu Rev Entomol* 59:165–184.
- Pliske TE. 1975a. Courtship behavior and use of chemical communication by males of certain species of ithomiine butterflies (Nymphalidae: Lepidoptera). *Ann Entomol Soc Am* 68:935–942.
- Pliske TE. 1975b. Courtship behavior of the monarch butterfly, *Danaus plexippus* L. *Ann Entomol Soc Am* 68:143–151.
- Pliske TE, Edgar JA, Culvenor CCJ. 1976. The chemical basis of attraction of ithomiine butterflies to plants containing pyrrolizidine alkaloids. *J Chem Ecol* 2:255–262.
- Raguso RA, Willis MA. 2005. Synergy between visual and olfactory cues in nectar feeding by wild hawkmoths, *Manduca sexta*. *Anim Behav* 69:407–418.
- Ramdyia P, Benton R. 2010. Evolving olfactory systems on the fly. *Trends Genet* 26:307–16.
- Ray A, van der Goes, van Naters W, Carlson JR. 2008. A regulatory code for neuron-specific odor receptor expression. *PLoS Biol* 6:e125.
- Regier JC, Mitter C, Zwick A, Bazinet AL, Cummings MP, Kawahara AY, Sohn J-C, Zwickl DJ, Cho S, Davis DR, Baixeras J, Brown J, Parr C, Weller S, Lees DC, Mitter KT. 2013. A large-scale, higher-level, molecular phylogenetic study of the insect order Lepidoptera (moths and butterflies). *PLoS One* 8:e58568.
- Rø H, Müller D, Mustaparta H. 2007. Anatomical organization of antennal lobe projection neurons in the moth *Heliothis virescens*. *J Comp Neurol* 500:658–675.
- Rospars JP. 1983. Invariance and sex-specific variations of the glomerular organization in the antennal lobes of a moth, *Mamestra brassicae*, and a butterfly, *Pieris brassicae*. *J Comp Neurol* 220:80–96.
- Rospars JP, Hildebrand JG. 1992. Anatomical identification of glomeruli in the antennal lobes of the male sphinx moth *Manduca sexta*. *Cell Tissue Res* 270:205–227.
- Rutowski RL. 1984. Sexual selection and the evolution of butterfly mating behaviour. *J Res Lepid* 23:125–142.
- Sandoz J-C, Deisig N, de Brito Sanchez MG, Giurfa M. 2007. Understanding the logics of pheromone processing in the honeybee brain: from labeled-lines to across-fiber patterns. *Front Behav Neurosci* 1:5.
- Schachtner J, Schmidt M, Homberg U. 2005. Organization and evolutionary trends of primary olfactory brain centers in Tetraconata (Crustacea + Hexapoda). *Arthropod Struct Dev* 34:257–299.
- Scotland RW. 2010. Deep homology: a view from systematics. *BioEssays* 32:438–449.
- Scott JA. 1973. Mating of butterflies. *J Res Lepid* 11:99–127.
- Silbering AF, Rytz R, Grosjean Y, Abuin L, Ramdyia P, Jefferis GSXE, Benton R. 2011. Complementary function and integrated wiring of the evolutionarily distinct *Drosophila* olfactory subsystems. *J Neurosci* 31:13357–13375.
- Sjöholm M, Sinakevitch I, Ignell R, Strausfeld NJ, Hansson BS. 2005. Organization of Kenyon cells in subdivisions of the mushroom bodies of a lepidopteran insect. *J Comp Neurol* 491:290–304.
- Skiri HT, Rø H, Berg BG, Mustaparta H. 2005. Consistent organization of glomeruli in the antennal lobes of related species of heliothine moths. *J Comp Neurol* 491:367–380.
- Snell-Rood EC, Papaj DR, Gronenberg W. 2009. Brain size: a global or induced cost of learning? *Brain Behav Evol* 73:111–128.
- Stephan H, Frahm H, Baron G. 1981. New and revised data on volumes of brain structures in insectivores and primates. *Folia Primatol* 35:1–29.
- Strausfeld NJ. 2012. *Arthropod brains: evolution, functional elegance, and historical significance*. Cambridge, MA: Belknap Press of Harvard University Press.
- Strausfeld NJ, Li Y. 1999. Organization of olfactory and multimodal afferent neurons supplying the calyx and pedunculus of the cockroach mushroom bodies. *J Comp Neurol* 409:603–625.
- Strausfeld NJ, Hansen L, Li Y, Gomez RS, Ito K. 1998. Evolution, discovery, and interpretations of arthropod mushroom bodies. *Learn Mem* 5:11–37.
- Strausfeld NJ, Sinakevitch I, Brown SM, Farris SM. 2009. Ground plan of the insect mushroom body: functional and evolutionary implications. *J Comp Neurol* 513:265–291.
- Streiner M, Kelber C, Pfabigan S, Kleineidam CJ, Spaethe J. 2013. Sexual dimorphism in the olfactory system of a solitary and a eusocial bee species. *J Comp Neurol* 521:2742–2755.
- Striedter GF. 2005. *Principles of brain evolution*. Sunderland, MA: Sinauer Associates.
- Tamura K, Peterson D, Peterson N, Stecher G, Nei M, Kumar S. 2011. MEGA5: molecular evolutionary genetics analysis using maximum likelihood, evolutionary distance, and maximum parsimony methods. *Mol Biol Evol* 28:2731–2739.
- Team RDC. 2008. R: a language and environment for statistical computing. Vienna, Austria: R Foundation for Statistical Computing. <http://www.R-project.org>.
- Theobald JC, Warrant EJ, O'Carroll DC. 2010. Wide-field motion tuning in nocturnal hawkmoths. *Proc Biol Sci* 277:853–860.
- Todd JL, Anton S, Hansson BS, Baker TC. 1995. Functional organization of the macroglomerular complex related to behaviourally expressed olfactory redundancy in male cabbage looper moths. *Physiol Entomol* 20:349–361.
- Topper CP. 2009. Nocturnal behaviour of adults of *Heliothis armigera* (Hübner) (Lepidoptera: Noctuidae) in the Sudan Gezira and pest control implications. *Bull Entomol Res* 77:541.
- Trigo JR, Motta PC. 1990. Evolutionary implications of pyrrolizidine alkaloid assimilation by danaine and ithomiine larvae (Lepidoptera: Nymphalidae). *Experientia* 46:332–334.
- Trona F, Anfora G, Bengtsson M, Witzgall P, Ignell R. 2010. Coding and interaction of sex pheromone and plant volatile signals in the antennal lobe of the codling moth *Cydia pomonella*. *J Exp Biol* 213:4291–4303.
- Trona F, Anfora G, Balkenius A, Bengtsson M, Tasin M, Knight A, Janz N, Witzgall P, Ignell R. 2013. Neural coding merges sex and habitat chemosensory signals in an insect herbivore. *Proc R Soc B* 280:20130267.

- Varela N, Couton L, Gemenio C, Avilla J, Rospars J-P, Anton S. 2009. Three-dimensional antennal lobe atlas of the oriental fruit moth, *Cydia molesta* (Busck) (Lepidoptera: Tortricidae): comparison of male and female glomerular organization. *Cell Tissue Res* 337:513–526.
- Vasconcelos-Neto J, Brown KS Jr. 1982. Interspecific hybridization in *Mechanitis* butterflies (Ithomiinae): a novel pathway for the breakdown of isolating mechanisms. *Biotropica* 288–294.
- Wahlberg N. 2006. That awkward age for butterflies: insights from the age of the butterfly subfamily Nymphalinae (Lepidoptera: Nymphalidae). *Syst Biol* 55:703–714.
- Walters JR, Stafford C, Hardcastle TJ, Jiggins CD. 2012. Evaluating female remating rates in light of spermatophore degradation in *Heliconius* butterflies: pupal-mating monandry versus adult-mating polyandry. *Ecol Entomol* 37:257–268.
- Wanner KW, Anderson AR, Trowell SC, Theilmann DA, Robertson HM, Newcomb RD. 2007. Female-biased expression of odourant receptor genes in the adult antennae of the silkworm, *Bombyx mori*. *Insect Mol Biol* 16:107–119.
- Wei H, el Jundi B, Homberg U, Stengl M. 2010. Implementation of pigment-dispersing factor-immunoreactive neurons in a standardized atlas of the brain of the cockroach *Leucophaea maderae*. *J Comp Neurol* 518:4113–4133.
- Withers GS, Fahrbach SE, Robinson GE. 1993. Selective neuroanatomical plasticity and division of labour in the honeybee. *Nature* 364:238–240.
- Xia Q, Zhou Z, Lu C, Cheng D, Dai F, Li B, Zhao P, Zha X, Cheng T, Chai C, Pan G, Xu J, Liu C, Lin Y, Qian J, Hou Y, Wu Z, Li G, Pan M, Li C, Shen Y, Lan X, Yuan L, Li T, Xu H, Yang G, Wan Y, Zhu Y, Yu M, Shen W, Wu D, Xiang Z, Yu J, Wang J, Li R, Shi J, Li H, Li G, Su J, Wang X, Li G, Zhang Z, Wu Q, Li J, Zhang Q, Wei N, Xu J, Sun H, Dong L, Liu D, Zhao S, Zhao X, Meng Q, Lan F, Huang X, Li Y, Fang L, Li C, Li D, Sun Y, Zhang Z, Yang Z, Huang Y, Xi Y, Qi Q, He D, Huang H, Zhang X, Wang Z, Li W, Cao Y, Yu Y, Yu H, Li J, Ye J, Chen H, Zhou Y, Liu B, Wang J, Ye J, Ji H, Li S, Ni P, Zhang J, Zhang Y, Zheng H, Mao B, Wang W, Ye C, Li S, Wang J, Wong GK-S, Yang H. 2004. A draft sequence for the genome of the domesticated silkworm (*Bombyx mori*). *Science* 306:1937–1940.
- Zhan S, Merlin C, Boore JL, Reppert SM. 2011. The monarch butterfly genome yields insights into long-distance migration. *Cell* 147:1171–1185.